



Alain Thien Tran, B.Eng.

Auslegung einer Apparatur zur Verschleißbeurteilung von Walzwerkstoffen

MASTERARBEIT

zur Erlangung des akademischen Grades

Diplom-Ingenieur

Masterstudium Advanced Materials Science

eingereicht an der

Technischen Universität Graz

Betreuer

Univ.-Prof. Dipl.-Ing. Dr.techn., Christof, Sommitsch

IMAT - Institute of Materials Science, Joining and Forming

Dr. Master, Coline, Béal

Danksagung

Da dies für mich persönlich der wichtigste Eintrag der Masterarbeit ist, möchte ich mir an dieser Stelle die Freiheit nehmen allen, die mir während des Studiums zur Seite standen zu danken und dem Leser einige persönliche Dinge mitzuteilen.

Großer Dank gebührt Prof. Sommitsch, Coline Béal, Armin Paar und allen beim IMAT Institut und ESW, die es mir überhaupt erst möglich gemacht haben dieses herausfordernde Projekt anzutreten und mir immer mit Geduld und Hilfe zur Seite standen. Ebenfalls meinen Eltern, die mich auf dem akademischen Weg gebracht haben. Als Migrationskind zweiter Generation ist dies leider heutzutage immer noch nicht selbstverständlich, aber ich hoffe, dass ich dadurch auch anderen den Mut gebe diesen Weg anzutreten. Ebenfalls zur Seite stand mir immer mein Bruder, der einen ähnlichen Weg wie ich bestreitet hat und auf den ich stets unglaublich stolz bin. Meinen besten Freunden René und Wei, die mir immer Ratschläge für das ganze Leben geben, bin ich ebenfalls zu Dank verpflichtet – ich hoffe ihr werdet auf eure Errungenschaften ebenfalls stolz sein. Omar und Ahmed – meine Studienkollegen – danke ich vielmals für Ihre Hilfe beim Studium wann immer ich sie benötigt habe. Und zu letzt meine Verlobte Isabel, die mir immer die Kraft gegeben hat auch in harten Zeiten auszuharren und immer nach vorne zu blicken. Ihr verdanke ich den Rückhalt, der mir täglich mit ihrer Liebe und Freude neue Energie gegeben hat.

Zuletzt möchte ich die Arbeit allen Menschen widmen, die es – sei es finanziell, gesundheitlich, kulturell o.ä. - nicht leicht im Leben hatten. Ich hoffe, dass ich dadurch diesen Menschen ein Beispiel setzen kann euer Ziel zu verfolgen, egal wie schwierig oder aussichtslos der Weg dahin manchmal sein kann. Auch wenn viele sagen, ihr schafft es nicht – glaubt an euch selbst und zeigt, dass ihr es dennoch könnt. Und mit den Worten, die mir meine Mutter einmal mitgegeben hat, möchte ich hiermit zum Abschluss kommen: „Es kommt der Tag, an dem du nicht bereust was du getan hast, sondern was du nicht getan hast.“

Acknowledgements

This entry will be personally the most important part of my master thesis, which is why I would like to take the freedom of thanking everyone who helped me during my master program. Also, I would like to share my personal thoughts to everyone who reads this.

I send big gratitude to Prof. Sommitsch, Coline Béal, Armin Paar and everyone at the IMAT institute and ESW who made it even possible for me to take such a challenging project and who were always patiently and helpful by my side. I thank my parents for leading me into an academic path. Sadly, for a second generation migrate this is still not common but I hope that with this I can give other people to do so. My brother who also walked a similar path like me and who I am very proud of each day. I also am deeply thankful to my best friends René and Wei, who are always giving me advice in my life – I hope you will also be proud of your achievements. My colleagues Omar and Ahmed also have my gratitude for helping me with the program whenever I needed their help. And last but not least my fiancé Isabel, who always gave me strength to endure hard times and told me to always look forward. Because of her love and support she was always able to give me the energy to go on.

Finally, I would like to devote this thesis to all the people who had hard times: Financially, for health reasons, culturally, etc. I hope I can be an example to always pursuit your goals no matter how difficult. Even though if people are saying that you cannot do it – believe in yourself and show them that you can do it. The end of this entry will be marked by some words my mother once told me: “The day will come, where you will not regret the things you did, but the things you did not do.”

Eidesstattliche Erklärung

Ich erkläre an Eides statt, dass ich die vorliegende Arbeit selbstständig verfasst, andere als die angegebenen Quellen/Hilfsmittel nicht benutzt, und die den benutzten Quellen wörtlich und inhaltlich entnommenen Stellen als solche kenntlich gemacht habe. Das in TUGRAZonline hochgeladene Textdokument ist mir der vorliegenden Masterarbeit identisch

Statutory declaration

I declare that I have authored this thesis independently, that I have not used other than the declared sources/resources, and that I have explicitly marked all material which has been quoted either literally or by content from the use sources. The document which is uploaded on TUGRAZonline is identical with this master thesis.

July 2017

Signature

Kurzfassung

Hohe Qualität und Quantität sind heutzutage ein wichtiges Maß um in der Industrie konkurrenzfähig zu sein. Langlebigkeit, Zuverlässigkeit und Umweltverträglichkeit der Bauteile spielen bei der Produktion spielen eine wichtigere Rolle denn je. Im Falle des Warmwalzens fehlt es jedoch an einer einheitlichen Vorhersage der Abnutzung von Warmwalzen. Produkte wie Bleche für die Automobileindustrie, Bauindustrie u.a. hängen maßgeblich von deren Qualität ab.

Das Eisenwerk Sulzau-Werfen befasst sich mit der Produktion von Warmwalzen für verschiedene Industriezweige. Eines ihrer Ziele ist es, den genauen Abnutzungsgrad von Warmwalzen bestimmen zu können, so dass das ESW und die produzierenden Betriebe bereits im Voraus wissen, wann bestimmte Walzen ausgetauscht werden müssen.

Im Zuge dieser Masterarbeit wurde nun ein Prüfstand entwickelt, der den Verschleiß von verschiedenen Walzen simulieren und dadurch den Materialabtrag abhängig vom Volumen bestimmen kann. Dazu wurden verschiedene Konzepte von anderen wissenschaftlichen Arbeiten miteinander verglichen, um einen allgemeinen Entwurf für den zu entwickelnden Prüfstand zu erarbeiten.

Am Ende der Arbeit werden noch weitere Aussichten und Verbesserungsmöglichkeiten diskutiert, da dieses Projekt anhand einer zweiten Masterarbeit fortgeführt wird.

Abstract

Nowdays high quality and quantity of any products are important goals to be competitive in the industry. Longevity, reliability and environmental sustainability of components play a more important role than ever before. However, a unified determination of wear is missing in case of hot rolling processes. Products like sheets for the automobile industry, construction industry and others rely strongly on their quality.

The company Eisenwerk Sulzau-Werfen is dealing with the production of hot rolls for various sectors of the industry. One of the company's objective is to assess the wear behaviour of hot roll materials, so that ESW and other producing factories may know in advance when to change certain hot rolls.

Goal of this master thesis was the development of a device which is capable of simulating the hot rolling process and thus measuring the loss of material during this process. For that, different concepts from many scientific papers were compared and an overall design for that measurement device was proposed. In the end some outlooks and possible improvements are discussed because this project will be continued in a second master thesis.

Table of contents

Danksagung	2
Acknowledgements	3
Eidesstattliche Erklärung.....	4
Kurzfassung	5
Abstract	6
Table of contents	7
Abbreviations, formula symbols, indices	9
1 Introduction	10
2 Literature	11
2.1 History of forming	11
2.1.1 Classification of the forming process.....	11
2.1.2 Classification of the rolling process	12
2.2 Physical and mechanical processes during longitudinal rolling	13
2.2.1 Physical process.....	13
2.2.2 Mechanical process	14
2.3 Tribology	18
2.3.1 Definition.....	18
2.3.2 Friction	18
2.3.3 Lubrication.....	20
2.3.4 Wear.....	20
2.4 Contact mechanics – Hertzian contact stress	23
2.4.1 Hertzian contact theory	23
2.5 Research of existing methods	25
2.5.1 An investigation into the tribological behaviour of a work roll material at high temperature [5]	25
2.5.2 The wear of tool steel rolls during hot rolling of low carbon steels [6].....	26
2.5.3 Hot friction behaviour and wear behaviour of high speed steel and high chromium iron for rolls & Tribological behaviour of hot rolling rolls.....	28
2.5.4 Composition, Microstructure, Hardness, and Wear Properties of High-Speed Steel Rolls.	30
2.5.5 Laboratory and pilot mill scale evaluation methods for evaluating new work roll grade incorporating NDT methods [10]	31

Table of contents

2.5.6	Hot wear testing of roll alloys [11]	33
2.5.7	Basic Characteristics and Microstructure of High-carbon High Speed Steel Rolls for Hot Rolling Mill [12]	35
2.5.8	Development of new materials based on on-site and laboratory evaluation methods for understanding work roll surface degradation	36
2.5.9	Characteristics of high-speed tool as materials of work roll in hot rolling	37
2.5.10	Mechanisms of Surface Deterioration of Roll for Hot Strip Rolling [15]	39
2.5.11	Summary	39
3	Concept and development of the wear testing procedure	42
3.1	Definition of the task	42
3.2	ESW's testing factors and comparison to the researched testing factors	43
3.3	Concept of the hot roll measurement device and testing procedure	44
3.3.1	Concept drawing of the testing device	44
3.3.2	Testing procedure	45
3.4	Calculations	47
3.4.1	Hertzian pressure	47
3.4.2	Torque	48
3.5	Mechanical parts	48
3.5.1	Power unit	48
3.5.2	Bearing system	50
3.5.3	Force sensor	52
3.5.4	Screw linear actuator	52
3.5.5	Clutch/coupling	52
3.5.6	Induction heating	53
4	Results	54
4.1	Constructed device	54
4.2	Cost	56
5	Discussion of concept	57
6	Conclusion	58
7	Suggestions and outlook	59
	List of references	61
	List of figures	63
	Appendix	65

Abbreviations

ESW	Eisenwerk Sulzau-Werfen
Etc.	Et cetera
p.	page
HSS	High-speed steel
LST	Lateral-setting test
DIN	Deutsches Institut für Normung
ISO	International Standard Organization

1 Introduction

Research and development of working rolls are very complex processes where not only the ideal chemical composition needs to be found but also mechanical and physical properties such as hardness or temperature behaviour must be checked. Some of the hardest aspects in determining the quality of rolls are certainly the wear resistances. Various complex tribological phenomena make it difficult to determine the outcome of a roll's quality after development and the actual use during the production process.

To identify the wear of rolls in a simpler and more practical way for the industry, a concept of a wear measuring device, based on several scientific approaches, will be developed. This device can simulate the metal forming process of hot rolls, where all these different tribological wear phenomena like adhesive wear, abrasive wear, etc. occur. Besides the general testing process, different parts of the measurement device will be as well as their purpose. To find the best relation of quality and production cost of the device, some parts will need to be additionally purchased by other companies while other mechanical machine parts will be able to be produced independently (by the company itself or the TU Graz, producing mechanical parts). In the end the further development of the measurement device is discussed since this thesis will only include the development of the machine's concept. This discussion leads the way to further improve this concept and aim for a more reliable, realistic and accurate simulation of the rolling process. Ultimately it leads to a higher quality, a more efficient and a more ecological or rather economical rolling process which is a necessity in competing in today's high performance production segment.

2 Literature

2.1 History of forming

Historically the forming process has been processed and developed over millennia in different civilizations all over the world and is one of the oldest working techniques of mankind. Being one of the core procedure methods in metal processing it was one of the major steps in building tools, weapons, ship building, jewellery and many other objects. This led to forming being one of the core techniques of improved civilizations and set the base for crafting and trading. [1]

Up until today forming has become even more important in times of technological developments. Cars, household tools, complex buildings, aircrafts and many other things could not have been built with the continuous evolution of the metal forming process.

2.1.1 Classification of the forming process

“Forming is the name of the process due DIN 8580, in which a given raw material or work piece is transformed into another objective state of shaping. Particles are moved, so that the cohesive material and the mass stay unchanged. Forming can also be named plastic deformation.” (p. 397, translation by the author¹) [2]

Figure 2-1 shows the general classification of the forming process. According to the DIN 8582 forming can be categorized into the following groups:

- Compressive forming (Druckumformen DIN 8583)
- Combined tensile and compressive forming (Zugdruckumformen DIN 8584)
- Tensile forming (Zugumformen DIN 8585)
- Bending (DIN 8586)
- Shearing (DIN 8587)

¹ „Unter Umformen versteht man gemäß DIN 8580, eine gegebene Roh- oder Werkstoffstückform in eine bestimmte andere Zwischen- oder Fertigteilform zu überführen. Dabei werden die Stoffteilchen so verschoben, dass der Stoffzusammenhalt und die Masse unverändert bleiben. Das Umformen bezeichnete man früher auch als *plastische* oder *bildsame Formgebung*“. (translation by the author)

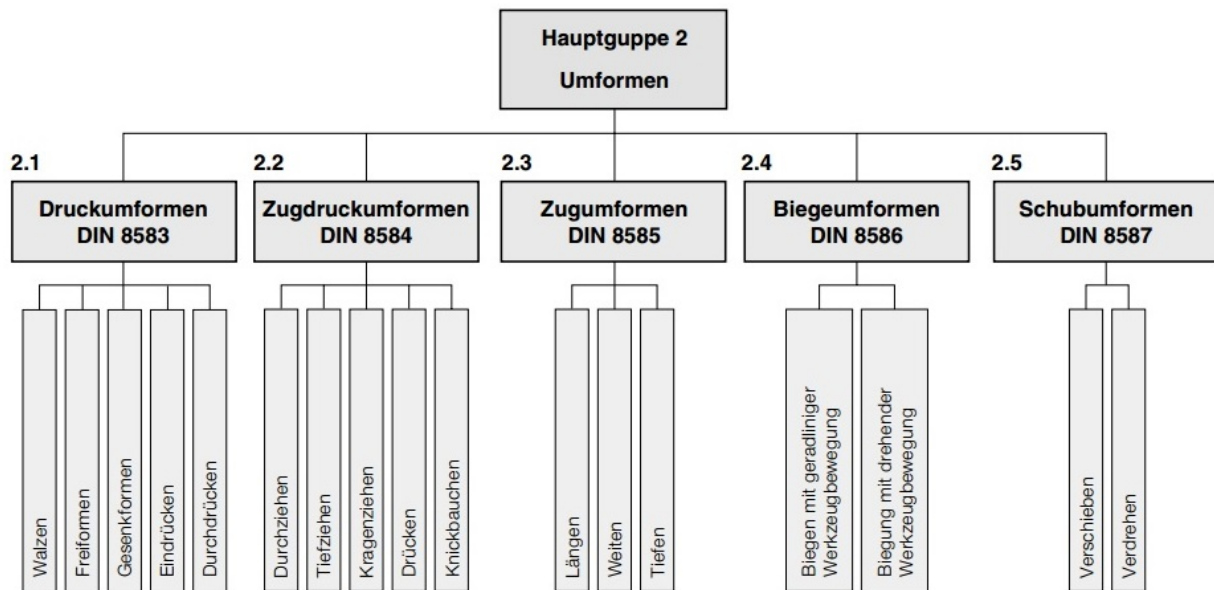


Figure 2-1: Classification of forming according to DIN 8582 [2]

Furthermore, compressive forming is also categorized into the following sub groups:

- Rolling
- Free forming
- Die forming
- Pressing
- Extrusion

2.1.2 Classification of the rolling process

“The process is defined as a continuous or gradual compressed forming with rotating tools (rolls).” (p. 406, translation by the author²) [2]

Figure 2-2 shows the classification of rolling processes according to DIN 8583. Generally, one can also distinguish the different rolling procedures due to the processing temperature which can be below or above the recrystallization temperature $T_{\text{recrystallization}}$:

- Hot rolling process: $T_{\text{process}} > T_{\text{recrystallization}}$
- Cold rolling process: $T_{\text{process}} < T_{\text{recrystallization}}$

² „Das Verfahren ist definiert als stetiges oder schrittweises Druckumformen mit sich drehenden Werkzeugen (Walzen).“ (translation by the author)

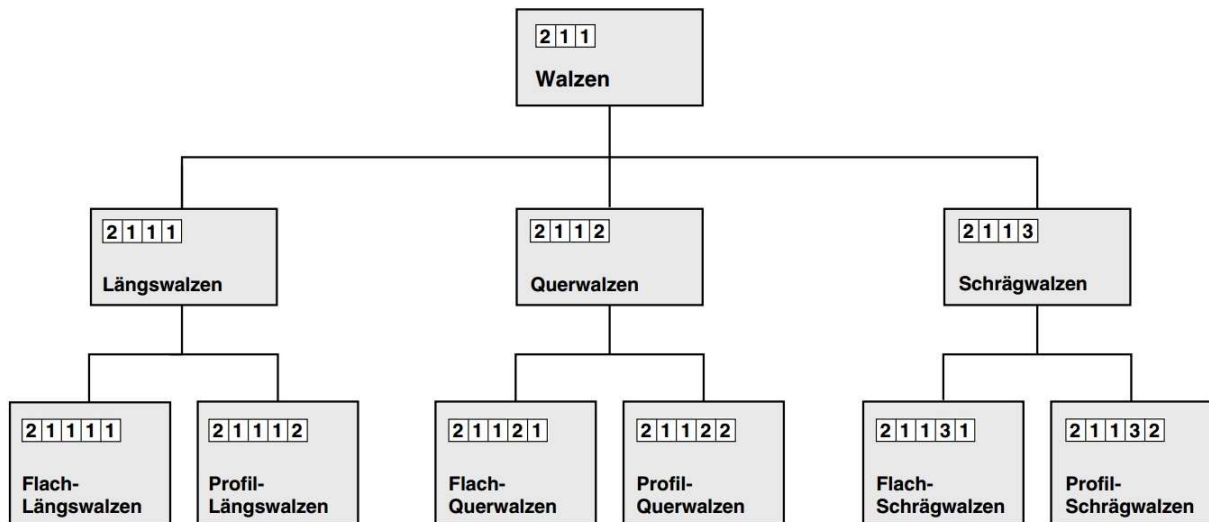


Figure 2-2: Classification of rolling according to DIN 8583 [2]

For the project, longitudinal rolling will be the base of the research and the simulation so other rolling techniques will be ignored.

2.2 Physical and mechanical processes during longitudinal rolling

2.2.1 Physical process

To understand the occurring physical phenomena during metal forming processes, a basic understanding of the atomic crystal structure is necessary. The structure of a metal can generally be described in three most common basic forms:

- Simple cubic
- Tetragonal
- Hexagonal

The properties of a material depend on the type/size of the atoms, their position and their distance. In general, plastic deformation can be explained due to the densest planes that parallelly slip on each other which is shown in **Figure 2-3**. In contrary to the isotropic behavior of these crystal structures an isotropic material behavior occurs in polycrystals because of their different and mixed structure where the slip planes can have different orientations.

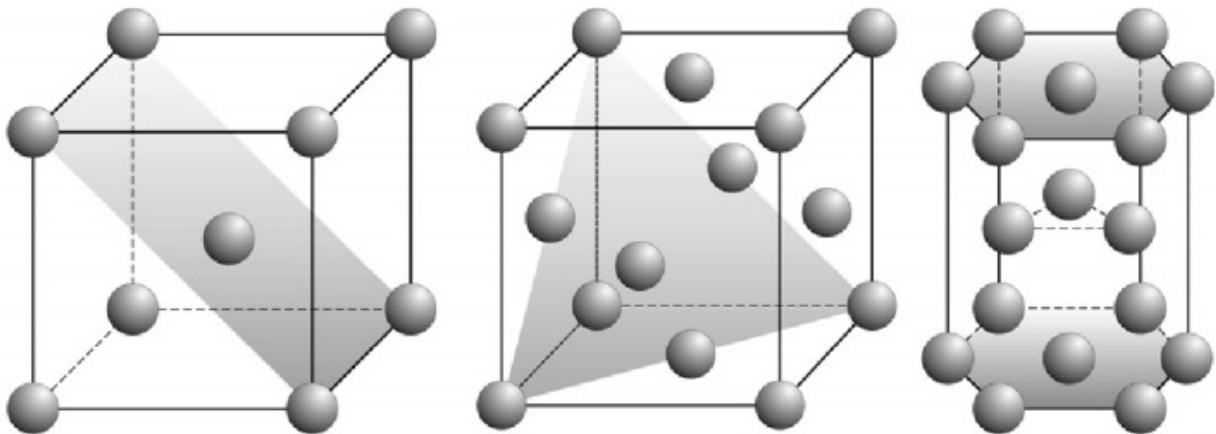


Figure 2-3: Unicell structure of metals: Body-centered cubic (left), face-centered cubic (center), hexagonal closed-packed (right) [2]

2.2.2 Mechanical process

In longitudinal rolling (sheet rolling) metal stock is passing through a pair of two or more rolls where its thickness is reduced after the forming between those rolls. The rolls can be of the same size but may also differ if needed. **Figure 2-4** illustrates the procedure and shows the different usage of more than two rolls.

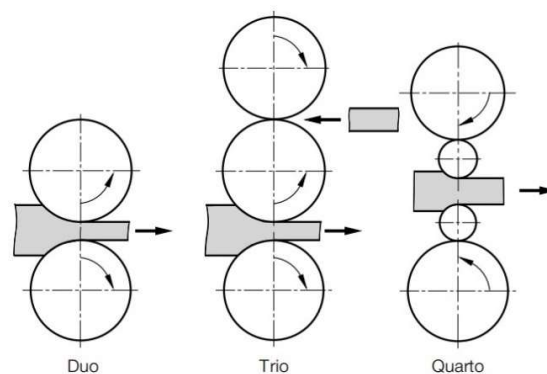


Figure 2-4: Illustration of duo, trio or quarto rolling systems [2]

As **Figure 2-4** shows, several roll arrangements can be used during the forming process. Depending on the force on the rolled raw material and the actual rolling process duo, trio or quarto systems can be used. Note that several other rolling systems are also available but are not mentioned here. In **Figure 2-5** several parameters describing rolling processes between the rolls and the raw material are shown:

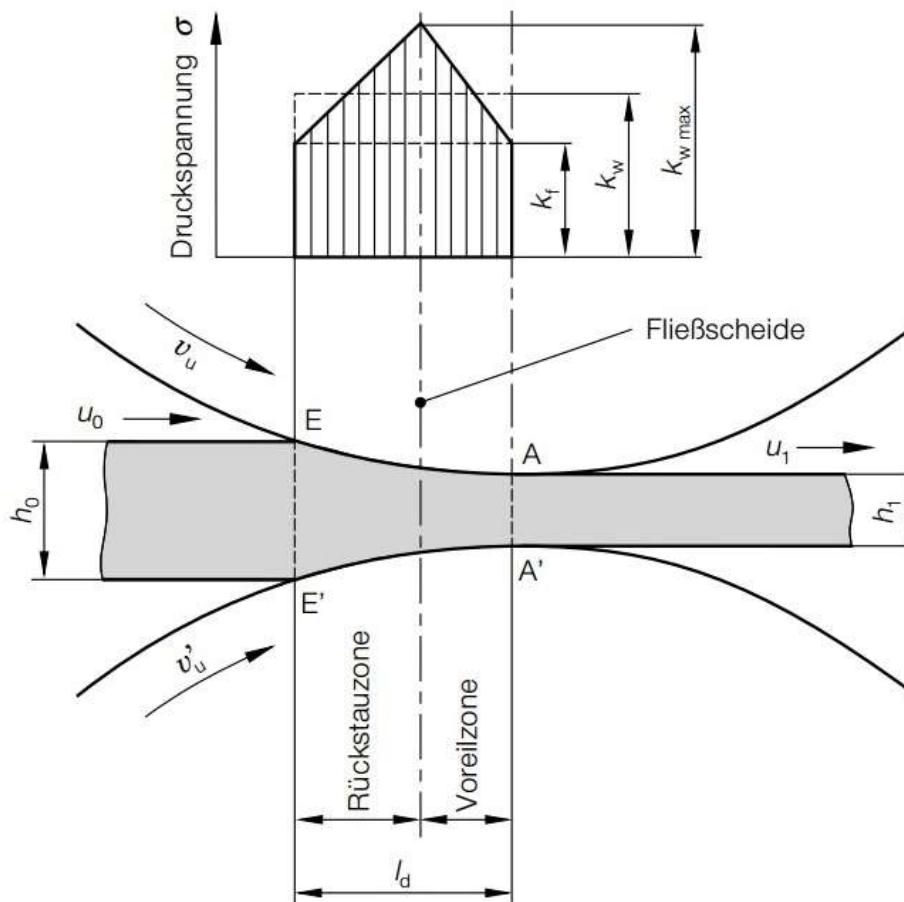


Figure 2-5: Parameters in longitudinal rolling with raw material between the rolls [2]

- v_u : Surface velocity of upper roll
- v'_u : Surface velocity of lower roll
- u_0 : Incoming velocity of the raw material/metal sheet
- u_1 : Outgoing velocity of the raw material/metal sheet
- h_0 : Initial thickness of the raw material/metal sheet
- h_1 : Resulting thickness of the raw material/metal sheet after rolling process
- $k_{w \max}$: Maximum resistance to deformation

It is essential to know that the incoming velocity of the incoming raw material/metal sheet is lower than the outgoing velocity ($u_0 < u_1$). The resulting thickness of the metal sheet is not only reduced from h_0 to h_1 with a thickness reduction $\Delta h = h_0 - h_1$, but the length of the sheet is also increased since the material needs to push the plastically deformed material into free spaces. At the “FlieBscheide” point the mean sheet velocity u_m equals the mean velocity v_m of the rolls. In

reality, an adhesion zone (“Haftzone”) is created due to the inhomogeneous flow of the material and increases with increasing adhesion of raw material and rolls (**Figure 2-6**).

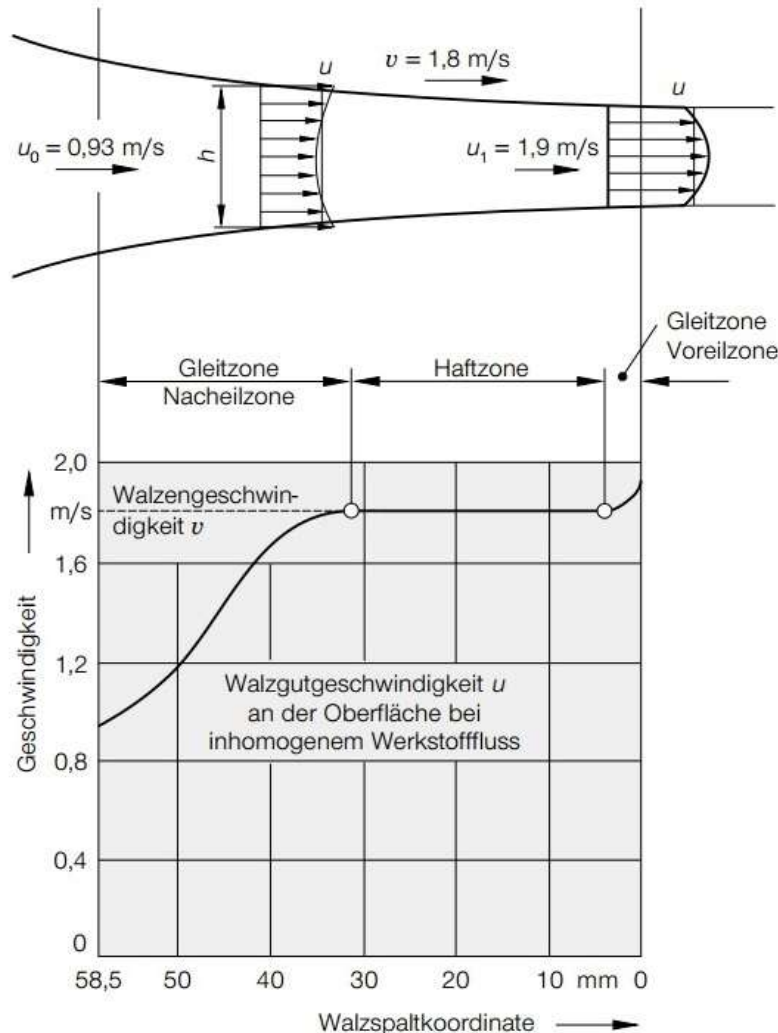


Figure 2-6: Velocity of the deformed metal sheet during forming process [2]

Importantly it can also be shown that friction also plays an important part with the kinematic of the material flow where the velocity of the raw material becomes constant in the “Haftzone” and the maximum friction is reached. The higher the friction becomes, the more the created “Haftzone” increases and thus the area where the material endures the highest compressive stress (maximum resistance to deformation). Thus, one can say that the “Fliescheide” area is the turning point where $u_0 < v$ changes into $u_1 > v$. [2]

The vertical rolling force F_w is shown in **Figure 2-7**.

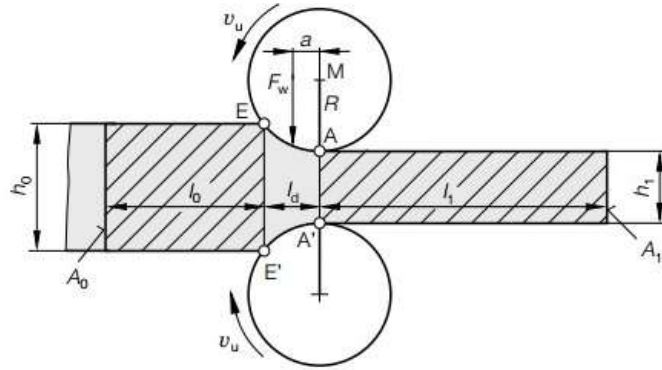


Figure 2-7: Vertical rolling force [2]

It is defined as

$$F_w = A_d k_w \quad (1)$$

$$F_w = A_d \frac{k_f}{\eta_F} \quad (2)$$

with k_f as the flow stress and k_w as resistance to deformation

$$\eta_F = \frac{k_f}{k_w} \quad (3)$$

and the compressed area A_d with the rolling radius R :

$$A_d = \sqrt{\Delta h R} \quad (4)$$

(4) in (1) leads to the equation:

$$F_w = \sqrt{\Delta h R} \frac{k_f}{\eta_F} = \sqrt{\Delta h R} k_w \quad (5)$$

F_w : Vertical rolling force

k_w : Resistance to deformation

k_f : Flow stress

A_d : Compressed area

R : Radius of rolls

Δh : Change of sheet thickness

η_F : Forming efficiency

2.3 Tribology

2.3.1 Definition

Tribology is defined as “science and technology of interacting surfaces in relative motion and the practices related thereto”. (p. E82) [3]

It describes the physical and chemical interplay between two bodies in contact. Since it is an essential engineering discipline in the rolling process the occurring phenomena are of an utmost importance. In general, there are three sections which are described by tribology:

- Friction
- Lubrication
- Wear

It is important to know that all three sections often occur at the same time which makes it often difficult to distinguish which one is of a dominating influence.

2.3.2 Friction

If two bodies which are in contact are moving relatively to each other friction occurs. It can be seen as an opposing force to the relative movement of the two bodies. The occurring forces are shown in **Figure 2-8** and consist of:

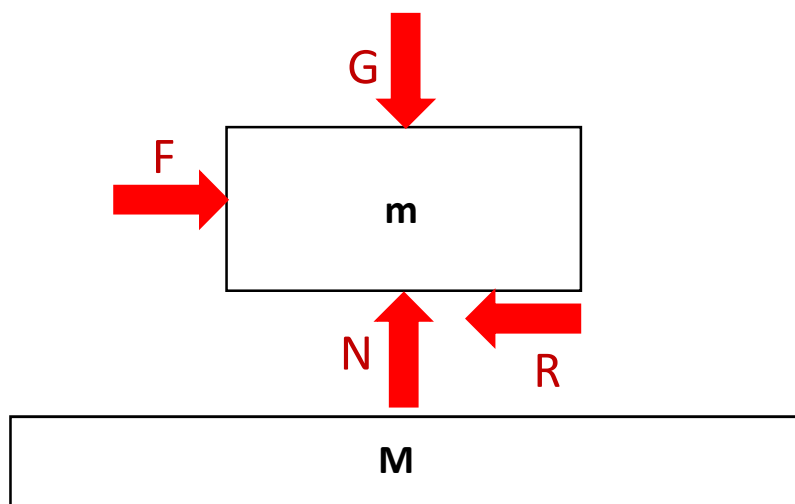


Figure 2-8: Mechanical forces on a body during friction

- Force of weight: $G = mg$ (6)

- Moving force F: $F = ma$ (7)

- Friction force R: $R = -F = -ma$ (8)

- Normal force N: $N = -G = -mg$ (9)

To get a relation between the vertical forces and the horizontal forces one can apply the friction law

$$R = \mu N \quad (10)$$

with μ being the nondimensional friction coefficient. It depends on different factors like the surface condition, type of material of both masses, lubrication, temperature and many others. Since steel is the main material in a rolling process the coefficient lies between 0,1 to 0,4. (p.255) [4]. In case of a hot rolling process there are three main cases which occur:

1. Slide friction

Slide friction occurs where two contacting bodies with different velocities are moving relatively to each other.

2. Rolling friction

The velocities of the bodies in contact are the same. In this case though, one body performs a rotatory motion on the second one. The contact areas can be point or line areas.

3. Mixed slide-rolling friction

Rolling friction with different velocities of two bodies (slippage).

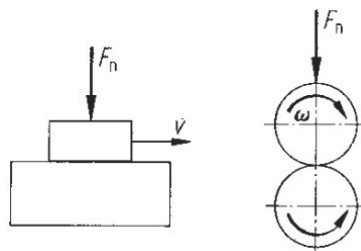


Figure 2-8: Slide friction (left) and rolling friction (right) [3]

Since the hot rolled strip moves in relation to the hot rolls during the forming process it will be set as the main friction event. It is noted that as a matter of course, additional friction phenomena as fluid friction, gas friction, etc. occur but are temporarily seen as not important for the construction.

2.3.3 Lubrication

The wearing device is developed in a “worse scenario case” which means the highest forces will be considered. Thus, lubricants that lower the friction forces will only be introduced briefly since very often the composition of the fluids must be adapted to the process with experiments and does not affect the construction at all.

Lubricants are fluids which lower the wear and the friction between two bodies where tribological phenomena occur. They form a film which lowers the friction coefficient since there is a metal-fluid-metal system. In the hot rolling process, they are also used for their cooling effects. Generally, there are three types of lubricants: (p. E85-E89) [3]

- Lubricant oils
- Lubricant greases
- Solid lubricants

The basic requirements for the lubricants in the hot rolling process such as lowering friction and wear, cooling (a defined heat capacity and conductivity for heat transport), being free of water to not support corrosion or protection against solid particles to lower abrasion behavior are all important factors that will be important for the experimental part of the wear measurement device project.

2.3.4 Wear

The DIN 50320 definition of wear describes it as an “[...] continuing loss of material from a solid’s surface, which origins are of mechanical cause, meaning contact and relative movements of a solid, fluid or gas antibody.” (p. E82, translation by the author)³ [3]

³ “Verschleiß ist der fortschreitende Materialverlust aus der Oberfläche eines festen Körpers, hervorgerufen durch mechanische Ursachen, d.h. Kontakt und Relativbewegung eines festen, flüssigen oder gasförmigen Gegenkörpers.“ (translation by the author)

Wear occurs if two surfaces move relatively or nonrelatively while contacting each other and is an undesirable effect. It can also be described as a loss of a body's mass where particles of the surface are broken off and its change of geometry leading to unwanted surface conditions which have negative impacts on the forming process. Typical reasons for this can be an insufficient thickness of the lubricant's fluid layer or systems with no lubricants at all. Bad surface conditions, high temperature, high forces, etc. also support the wear mechanism. Abrasion, adhesive wear, tribo-oxidation and surface fatigue wear are the major wear phenomena.

1. Abrasion wear

If a material is moving and rubbing on the surface of another material an abrasion occurs. In this case, micro chipping takes place and removes particles from the surface. The reason is due to the surfaces' roughness which mechanically enables cracking off particles when moving against each other. It is also essential to know that generally the harder surface rubs off the softer one but the softer material can also rub off the harder one. This case is called the two-body abrasive wear.

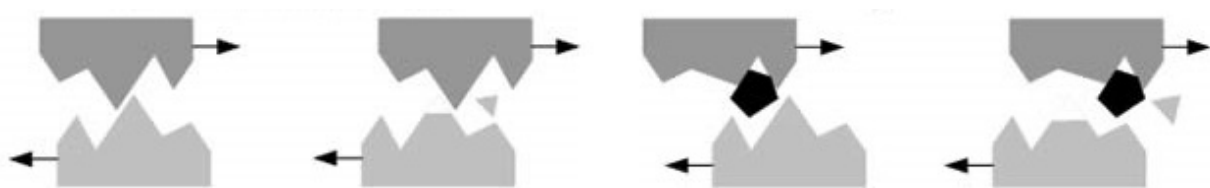


Figure 2-9: Abrasive wear – two-body (left), three-body (right)

Once a particle is removed from the surface it can stay in the gap between both materials and support further abrasion or is extracted from the system and moves out. Also, a third-party particle may also be included (for example due transportation through the lubrication fluid) and worsen the abrasive wear, too. In **Figure 2-9** it is illustrated how the rubbing motion of both surfaces cause particles to crack off either in a two-body or three-body system. Surfaces that suffered from abrasive wear often show grooves or cut gaps which show the direction of the relative movement. Abrasion can be lowered with surface treatments such as polishing or lubricants.

2. Adhesive wear

Due to the rubbing contact of the surfaces it is also possible that in certain areas regional joints are created due to micro welding processes. These fused contact points crack off again because of the surfaces' movements and induce additional loss of material (**Figure 2-10**).

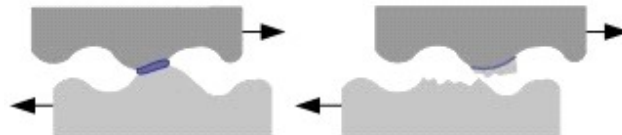


Figure 2-10: Adhesive wear of two surfaces

3. Tribo-oxidation

In addition to the mechanical wear processes a chemical wear process takes also place. Due to chemical reactions (corrosion/oxidation) of the surfaces with each other, the lubricants or its environment, this additional wear process causes a removal of particles from the surface. By choosing the proper lubricant it is possible to lower the tribo-oxidational wear.

4. Surface fatigue wear

Surface fatigue wear can be explained with a cyclic stress and load on the material where cracks are created because of the materials fatigue strength's transgression. After creating the cracks on the outer surface because of the periodic stress the cracks grow until they induce the material in those areas to breaking off.

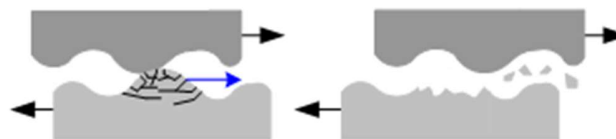


Figure 2-11: Surface fatigue wear

An illustration of the fatigue wear mechanism is shown in **Figure 2-11** where the break off is shown.

2.4 Contact mechanics – Hertzian contact stress

Contact mechanics is the most important base chapter for the hot rolling process since it sets the foundation of the wear device's concept. To simulate the real rolling process as close as possible different factors must be defined and calculated. These factors such as the pressuring force serve as a base for several parts that are included in the device of the hot rolls on the sample. Since the device is set in much smaller, laboratory-orientated scale than a real hot rolling device it is important to implement a correct stress on the material. With this the Hertzian contact stress theory will serve as a fundamental construct so the mechanical rolling processes can be simulated in a best possible way. The following chapter will describe the general model of two cylindrical objects that will be used later for the construction.

2.4.1 Hertzian contact theory

We take the case where an inelastic ball enters an elastic surface (**Figure 2-12**). Due to the inelastic property of the ball, it will enter the surface and deform the surface. The contact radius

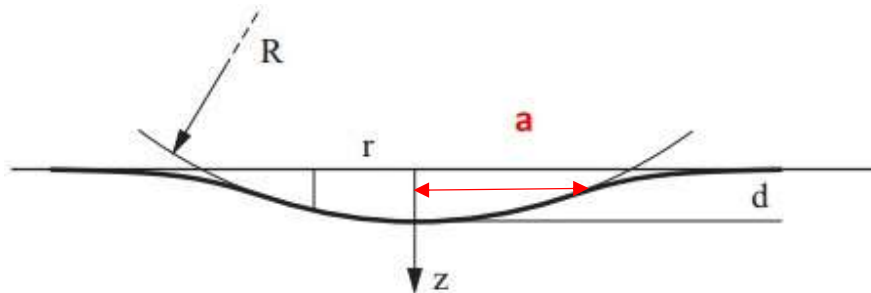


Figure 2-12: Inelastic ball entering an elastic room [5]

a is defined as half the distance between the touching points of the ball and the surface:

$$a^2 = Rd \quad (11)$$

where the maximal pressure p_0 can be calculated with the E-modulus:

$$p_0 = \frac{2}{\pi} E \sqrt{\frac{d}{R}} \quad (12)$$

If (12) is inserted into

$$F = \frac{2}{3} p_0 \pi a^2 \quad (13)$$

we get the force F that is used to push the ball into the surface:

$$F = \frac{4}{3}E\sqrt{R^3d} \quad (14)$$

Now we consider both bodies to be elastic, cylindrical and have parallel axes (**Figure 2-13**). In this

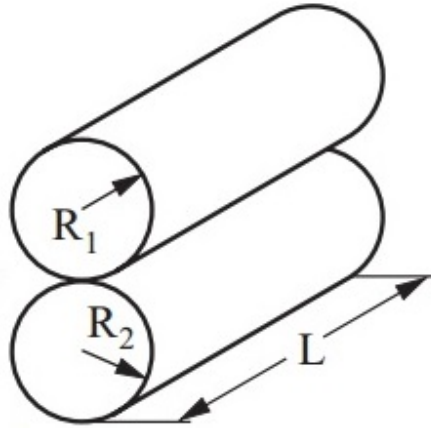


Figure 2-13: Two cylinders touching each other with parallel axes [5]

case E must be calculated with

$$\frac{1}{E} = \frac{1-\vartheta_1^2}{E_1} + \frac{1-\vartheta_2^2}{E_2} \quad (15)$$

where E_1 and E_2 are the different E-modulus and ϑ is the Poisson number of each body. The radii of both cylinders can also be merged into:

$$\frac{1}{R} = \frac{1}{R_1} + \frac{1}{R_2} \quad (16)$$

Since the force F aligns on a straight line between those two cylinders, equation (14) now changes:

$$F \approx \frac{\pi}{4}ELd \quad (17)$$

With the force F , we can finally get the Hertzian pressure p_0 : [5]

$$p_0 = \frac{2F}{\pi La} \approx \sqrt{\frac{EF}{\pi LR}} \quad (18)$$

2.5 Research of existing methods

To find a direction of the concept's development a research of various wear testing methods is necessary. Since there are not standardized methods and devices, the lack of experience makes it difficult to decide the optimum testing method. Another aspect is also the testing conditions which are also not set yet. Since laboratory testing differs from real rolling processes it is at utmost importance to get a direction of the testing factors. This chapter will briefly analyze several scientific methods and papers done by various institutions including Prof. Pellizzari's wear measurement device. The company ESW organized a trip to Trento to get a visual view on his device. It needs to be mentioned that the research's primary focus was the technical setup of the testing methods as the methods themselves. The composition of the samples or the test results are not mentioned.

2.5.1 An investigation into the tribological behaviour of a work roll material at high temperature [6]

For the experimental setting to investigate the oxidation behavior of high-speed steel (HSS) rolls a Gleeble 3500 was used as a base. The Gleeble is originally a material simulator system for tension, pressure or torsion tests with a heating system (additionally experimental setting parts for the atmosphere, quenching, etc. can be added, depending on the model). To simulate the hot

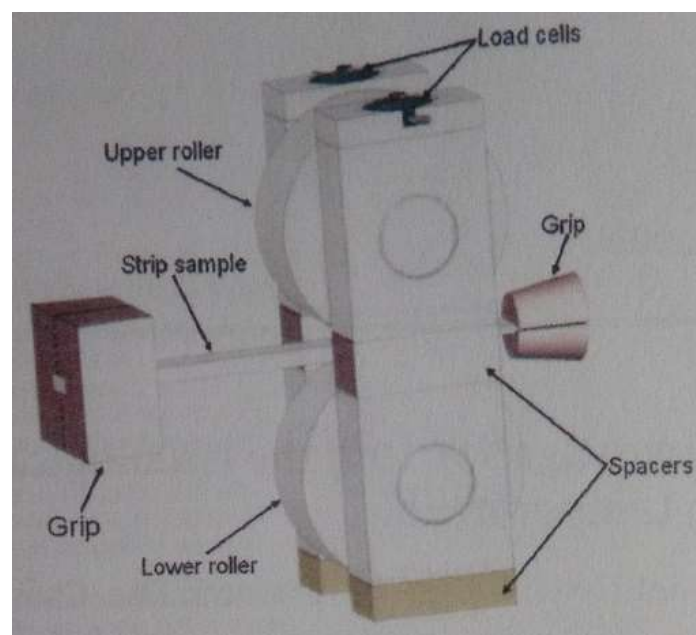


Figure 2-14: Illustration of mini two-high rolling mill [6]

rolling process, a mini two-high rolling mill – also called lateral-setting test (LST) - has been adapted and built in into the thermal-mechanical simulation system (**Figure 2-14**) and the Gleeble moves the strip between the rolls back and forth with the grip. The load can be changed due load cells which can be seen on top of the rig. To take influence on the thickness of the sample during the rolling process, spacers are installed that can be easily changed and thus the gap between the rolls can be regulated. [6]

Testing procedure:

The testing parameters were set up in the following way (**Table 2-15**):

Setup parameters	Values
Rolling speed	15 mm/s
Testing Temperature	700 – 850°C
Rolling force	15 – 45 kN
Roll diameter	50 mm
Testing atmosphere	Argon
Testing time	Not mentioned

Table 2-15: Testing setup parameters

The first step was to measure the strip sample's thickness before the rolling process. After that, the strip was heated up to the necessary temperature. Once the right temperature was achieved it was hot rolled with a rolling speed of 15 mm/s while the rolling force was measured online. The testing considerations after the hot forming process were the change of the strip sample's thickness and the surface roughness of the roll according to ISO 11562.

2.5.2 The wear of tool steel rolls during hot rolling of low carbon steels [7]

The university of Waterloo took a different approach by changing the setup of a Stanat laboratory rolling mill (**Figure 2-16**). For this configuration, the bottom work and back up rolls were removed. A sample holder with a wear specimen are placed in position where the rolls had been before. The wear specimen was made of hot rolled AISI 1018 steel and formed as a block (**Figure 2-17**).



Figure 2-16: Stanat rolling mill [7]

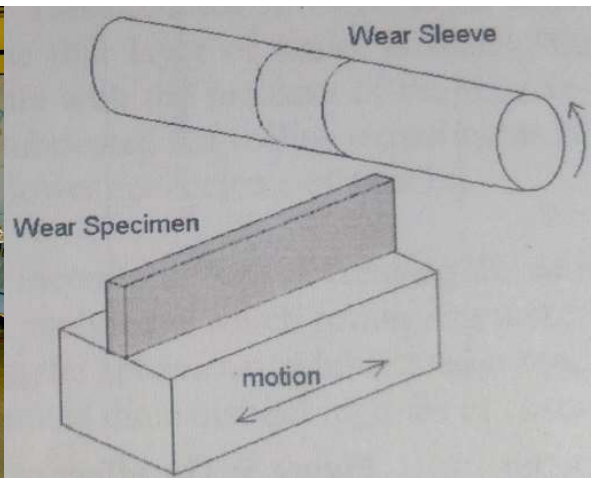


Figure 2-17: Illustration of the testing method [7]

A hollow cylinder/sleeve with a specific roughness and hardness, which was backed up by the upper roll, served as the testing hot roll (**Figure 2-17**) and two side torches could heat up the sample strip. [7]

Testing procedure:

The testing parameters were set up in the following way (**Table 2-18**):

Setup parameters	Values
Rolling speed	45 – 90 rpm (0,09 – 0,19 m/s)
Testing temperature	700 – 850 °C
Rolling force	150 – 300 N
Strip geometry	38 x 6,4 x 100 mm
Testing duration	1 st : 7 min, 2 nd : 10 min, 3 rd : 10 min

Table 2-18: Testing parameters

After determining the weight of the strip sample and the work roll, the sample was heated up to the desired temperature. Once the temperature was reached the rolls were set down until they touched the sample with the defined force and then start rolling while the sample holder would move the sample with a horizontal motion towards the roll's surface. once the first testing period was over, the mass of the roll and the strip was measured again before they would undergo a second and third testing procedure with a pro-longed testing time. It is also mentioned that the

force, temperature and the friction load were online measure during the whole testing procedure. A cooling of the work roll was also implemented.

2.5.3 Hot friction behaviour and wear behaviour of high speed steel and high chromium iron for rolls & Tribological behaviour of hot rolling rolls [8]

Prof. M. Pellizzari used an Amsler tribometer (**Figure 2-19**) to measure the wear of hot rolls. The



Figure 2-19: Amsler tribometer

tribometer is a device that has two disks which rotate on each other's surface – very similar to a real hot roll rig. An engine transmits a torque on 2 parallel drive shafts. On each end of a drive shaft a sample is mounted on. By turning a force screw, it is possible to vertically move to shafts closer to each other and thus setting the pressure between the two disks. The heating of the hot mill strap was done with an induction heating system and measured with an infrared pyrometer.

Figure 2-20 shows the test setting with the two-disk wear testing procedure. [8] [9]

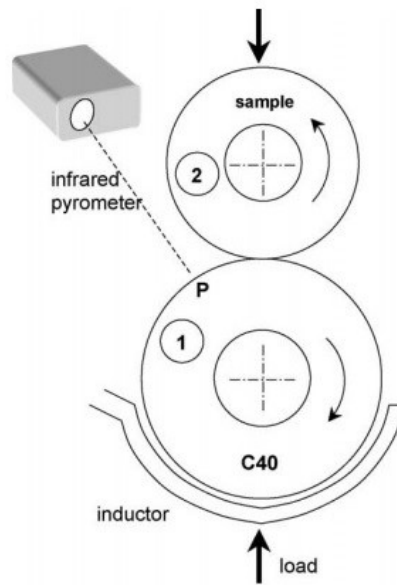


Figure 2-20: Setting of the hot rolling wear testing procedure

Testing procedure:

Setup parameters	Values
Rolling speed	180 & 200 rpm (0,47 & 0,52 m/s)
Slippage	28 %
Testing temperature	700 °C
Rolling force	300 N (~300 MPa Hertzian pressure)
Sample geometry	Hot strip roll: $d_a = 50$ mm, $b = 10$ mm Sample roll: $d_a = 40$ mm, $b = 10$ mm
Testing duration	3 x 60 min

Table 2-21: Testing parameters

Two disk shaped samples were weight before being fixed on the testing shaft. A surface roughness determination was also measured. One disk was the sample which represented the hot roll while the other was a C40 carbon steel disk that simulated the hot roll strip. The hot roll strip was heated up to 700 °C and left in this state for about 5 min to achieve oxidation. This was done because strips have a high temperature before being deformed in the factory process. The first testing period would take 60 min. After that the hot rolls sample was weight and a new C40 hot strip disk was also put on the shaft to assure a plain surface. A second and a third testing period with the

same length were added. For the whole testing procedure, a dry testing (no lubrication between the disks) was done.

2.5.4 Composition, Microstructure, Hardness, and Wear Properties of High-Speed Steel Rolls [10]

J. Paak, H. Lee and S. Lee approached the wear measurement in a very similar way as Prof. Pellizzari's method. Having used the same basic setting (**Figure 2-22**) the main difference were the water cooling of the hot roll disk and the different parameter settings. Additionally, by measuring the applied torque it was possible to calculate the friction coefficient using the equation: [10]

$$\mu = \frac{T}{PR} \quad (19)$$

μ : Friction coefficient

T: Torque [Nm]

P: Applied load on disks [MPa]

R: Radius of roll disk [mm]

The geometric drawing of the wear disk can be seen in **Figure 2-23**:

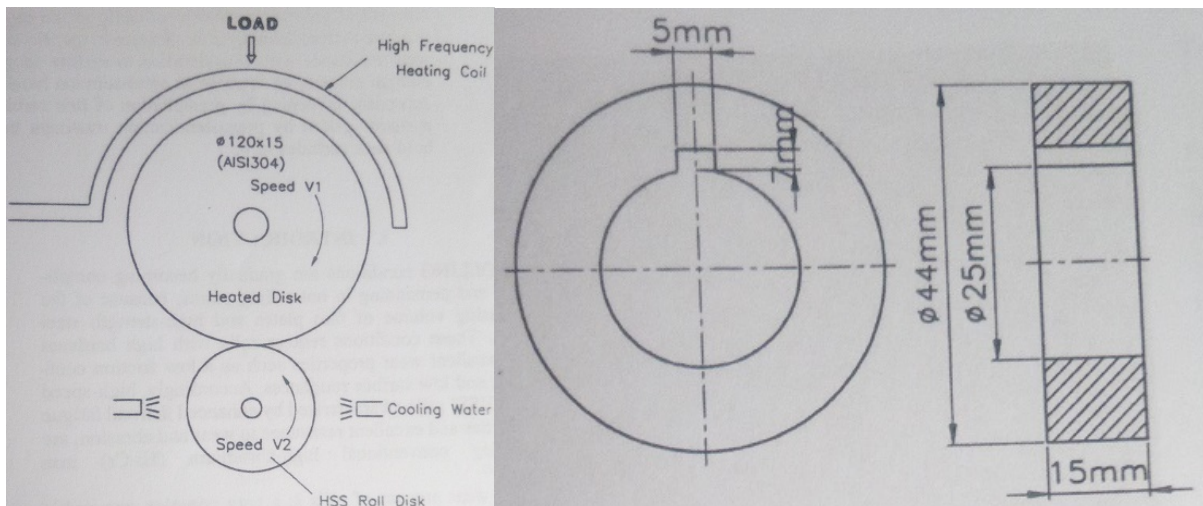


Figure 2-22: Setting of the wear test [10]

Figure 2-23: Geometric description of the wear disk [10]

Testing procedure:

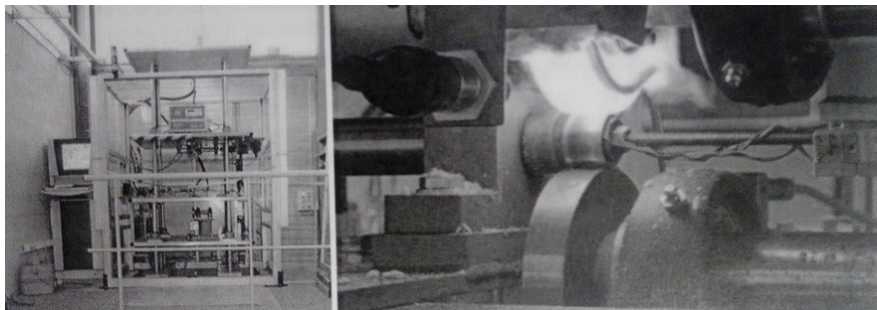
Setup parameters	Values
Rolling speed	0,3 m/s (130 rpm)
Slippage	34 %
Testing temperature	850 °C
Rolling force	600 MPa Hertzian pressure
Sample geometry	Wear roll: $d_a = 44$ mm, $d_i = 25$, $b = 15$ mm
Testing duration	12000 revolutions (92 min)

Table 2-24: Testing parameters

The experimental procedure would be similar to Prof. M. Pellizzari's tests. Two disks would be used: A C40 steel strip mill and a hot roll sample disk. Both had to be weight before they were fixed onto the device. The strip mill disk would also be heated up using a high frequency heating coil system. The hot roll disk on the other hand was cool with water. After pre-defined revolutions, the weight loss was measured and then documented. An online record of the disk speed, load and torque as in equation (19) was used for observation. The parameters were setup as in **Table 2-24**.

2.5.5 Laboratory and pilot mill scale evaluation methods for evaluating new work roll grade incorporating NDT methods [11]

Two different testing techniques were used by G. Walmag and J. Malbrancke. The first one was a three-disk system which consisted of a lower back-up roll, an upper hot strip and middle work roll disk with different dimensions. **Figure 2-25** shows the setup and the device was custom made.

**Figure 2-25:** Setup of the hot rolling simulation [11]

A temperature about 1100 °C was achieved due an induction heating while a cooling system was also available. Evaluation of the test results was performed with the measurement of the sample's surface degradation and metallographically. A second testing method allowed different samples during one testing period where a special "insert sample" roll was used (**Figure 2-26**) on a hot rolling pilot line. This sample roll enabled the implementation of six rectangular smaller samples.

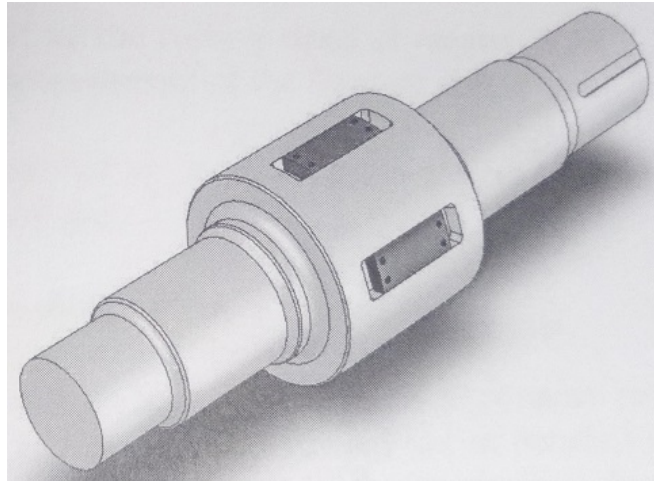


Figure 2-26: "Insert sample" work roll for six samples [11]

Using a complete hot rolling pilot line with a coilbox, a decoiler where the temperature for the strip could be set up, an inductive heater for additional temperature adjustment, mist cooling set, etc. the system was in general a reproduction of a real hot roll line.

Testing procedure:

Setup parameters	Values (Method 1)	Values (Method 2)
Rolling speed	-	-
Slippage	-	-
Testing temperature	1100 °C	1250 °C
Rolling force	-	-
Sample geometry	Back-up & Strip disk: $d_a = 120$ mm, $b = 20$ mm Work roll disk: $d_a = 30$ mm, $b = 10$ to 20 mm	Rectangular inserts: 175 x 75 x 30 mm
Testing duration	8 hours	Up to 7 trials (1 trial: 0,8 – 1,3 km)

Table 2-27: Testing parameters

Method 1 and 2 measured the roughness of the samples after certain testing periods. Additionally, a microscopic analysis could be done on the samples. The latter testing method implemented a parameter observation of the rolling data (force, temperature, speed and electrical current of the motor), the surface of the work with “rollscope”, the velocity of the outgoing strip at the exit of the rolling mill and the spindle torque. [11]

2.5.6 Hot wear testing of roll alloys [12]

Another disk on disk method used a hot wear testing device which was built and developed by Broken Hill Proprietary Research. Like former methods, two disks (a roll material and strip disk) are set in a parallel stage (**Figure 2-28**). Being heated by induction, the system had an additional water cooling system to achieve shaft temperatures under 30 °C due to the stray of the induction

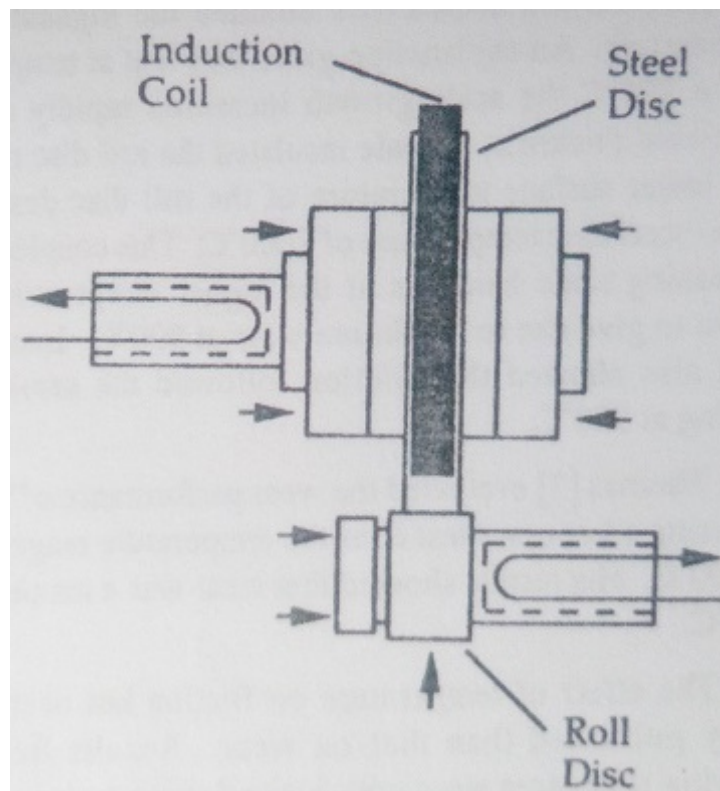


Figure 2-28: BHP testing rig [12]

fields. 2 kW AC-motors were used as power units for the shaft. The digital supervision of the rotations made any relative disk speed, slippage and change of direction possible. The roll disk additionally had a water-cooled copper nut, which kept the roll sample under 70 °C. A complete sealing system assured a closed atmospheric system. This could be used for example to do oxide

repressive testing procedures using gasses like argon etc. All the important parameters like temperature, disk speed, load, torque etc. were measured and supervised by in-house-made software. [12]

Testing procedure:

Setup parameters	Values
Rolling speed	-
Sliding distance/s	0,25 & 0,5 m/s
Testing temperature	900 °C
Rolling force	200 – 400 N
Sample geometry	b = 10 mm
Testing duration	-

Table 2-29: Testing parameters

The unique approach of wear was not the loss of mass in terms of volume but of total meter sliding distance. Equation (20) set up the definition of wear for this testing method:

$$W = \frac{w}{L} = \frac{w \pi D_1}{V_S b T} \quad (20)$$

W : Wear [mg/m]

w : Weight loss of roll disk [mg]

D_1 : Diameter of roll disk [m]

V_S : Slip ($V_1 - V_2$) [m/s]

b : Hertzian contact arc length [m]

T : Test duration [s]

The heated strip disks consisted of carbon steel to represent the deformed material.

2.5.7 Basic Characteristics and Microstructure of High-carbon High Speed Steel Rolls for Hot Rolling Mill [13]

Another testing procedure based on the roll profile and friction is shown in **Figure 2-30**:

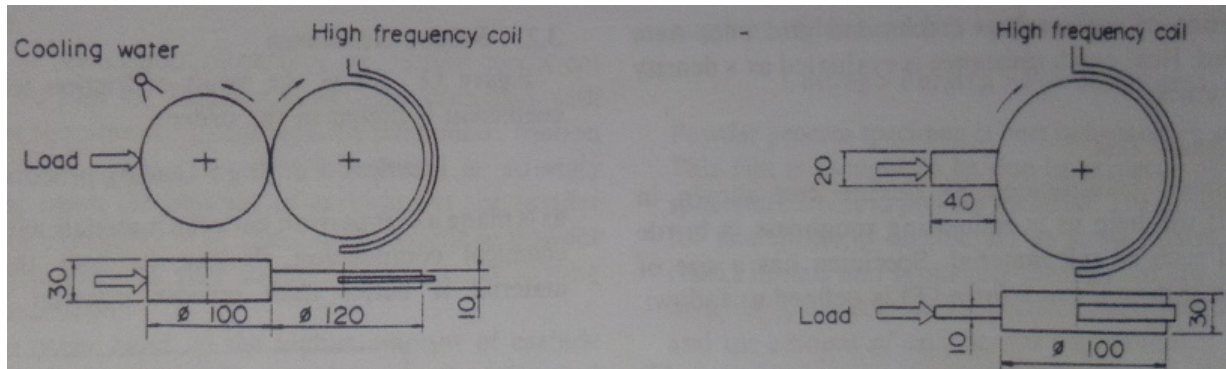


Figure 2-30: Wear test setting (left) and friction test setting (right) [13]

While the wear testing method used the already known two-disk method, the friction test method was built up in a block-disk system. [13]

Testing procedure:

Setup parameters	Wear test method	Friction test method
Rolling speed	1,05 m/s	0,05 m/s
Slippage	20 %	-
Testing temperature	700 °C	700 °C
Rolling force	350 MPa Hertzian pressure	100 MPa Hertzian pressure
Sample geometry	Strip disk: $d_a = 120$ mm $b = 10$ mm Work roll disk: $d_a = 100$ mm $b = 30$ mm	Strip disk: $d_a = 100$ mm $b = 30$ mm Work roll block: 20 x 40 x 10 mm
Testing duration	10000 cycles	60 s

Table 2-31: Testing parameters

For the wear test, a two-disk setting used a ASTM SUS304 made sample and heated up with a high frequency induction heating system. After the testing the profile of the specimen was measured with a 3D profile meter. Using equation (21)

$$dm = \frac{1}{N} \sum_{i=1}^N \frac{S_i}{W_i} \quad (21)$$

W_i : Width of wear profile

S_i : Cross sectional area of wear loss due to wear

N : Number of section measured

where the mean value dm of the wear depth could be calculated. For the friction test the samples were treated with acetone and ethanol first. After testing, the friction coefficient was determined with equation (19).

2.5.8 Development of new materials based on on-site and laboratory evaluation methods for understanding work roll surface degradation [14]

CRM group used a rolling simulator to evaluate the work roll degradation to backup and hot strip rolls independently. The rolling simulation device made it possible to switch between the testing methods. The first method to determine the influence of the hot strip on the work roll sample was done with a two-disk method (**Figure 2-32**).

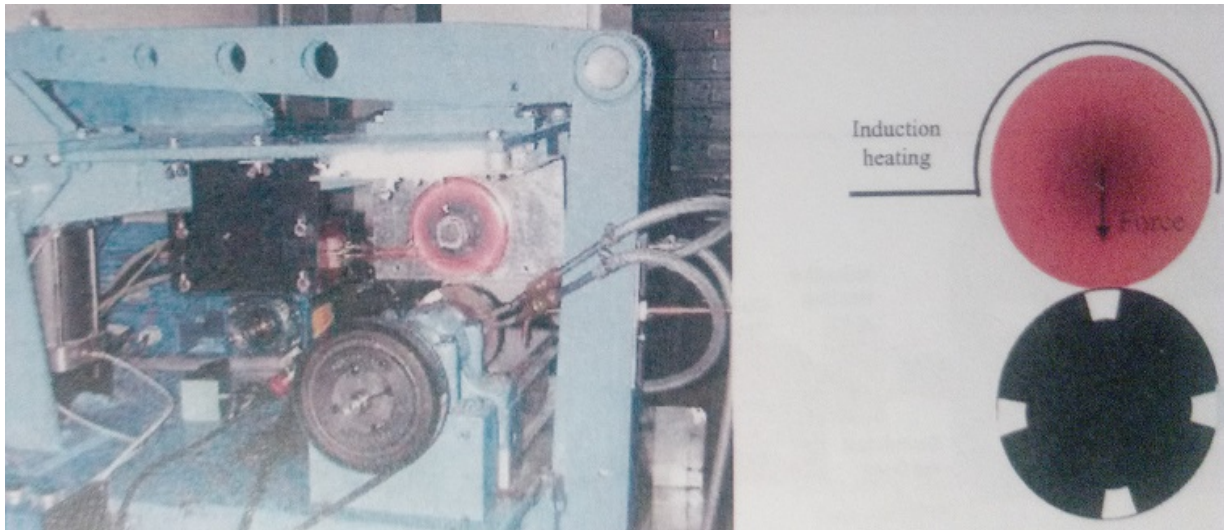


Figure 2-32: Two-disk hot strip testing setup [14]

Heating up the hot strip roll with an induction heater was included and an “insert sample” roll similar to **Figure 2-26** where four different inserts could be used. A three-disk setup was used to simulate the influence of the backup rolls on the sample. In this method two work rolls were being used (upper and bottom roll) where the force could be put on the upper disk (**Figure 2-33**). Cooling

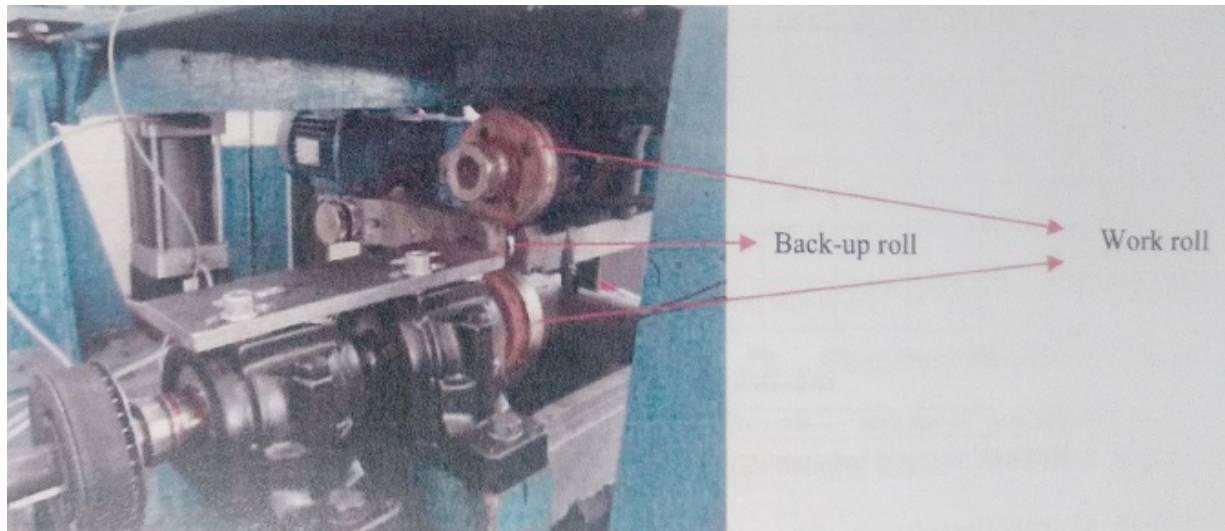


Figure 2-33: Three-disk back-up roll testing setup [14]

with sprayed water was also applied on the same work roll to simulate the industrial process. Temperature and composition of the cooling fluid could be adjusted. The influence of the strip and back-up rolls was measured with roughness, profile as well as a photo a microscopic examination. Lastly CRM also performed material tests on a real hot rolling mill street using “insert sample” roll for five samples. It is important that one sample’s grade is known to have a good comparison and survey to the other specimens. [14]

Testing procedure:

No useful testing parameters for the wear measurement device were mentioned.

2.5.9 Characteristics of high-speed tool as materials of work roll in hot rolling [15]

Nippon steel measured the wear W , the friction coefficient μ and adhesion resistance with a two-disk device which had different parameter values for the hot wear and adhesion resistance test. As a hot strip roll material S45C was used for the simulation in a hot wear tester (**Figure 2-34**) which was rubbing on the hot roll sample. For the adhesion resistance testing method the slippage was measured until adhesion would start appearing on the surface of the hot roll disk. Cooling on the hot roll sample was initialized with water coming out from attached nozzles. A high frequency induction heating coil around the hot strip disk heated it up for the testing. The pressure was applied from the upper strip disk onto the hot roll. [15]

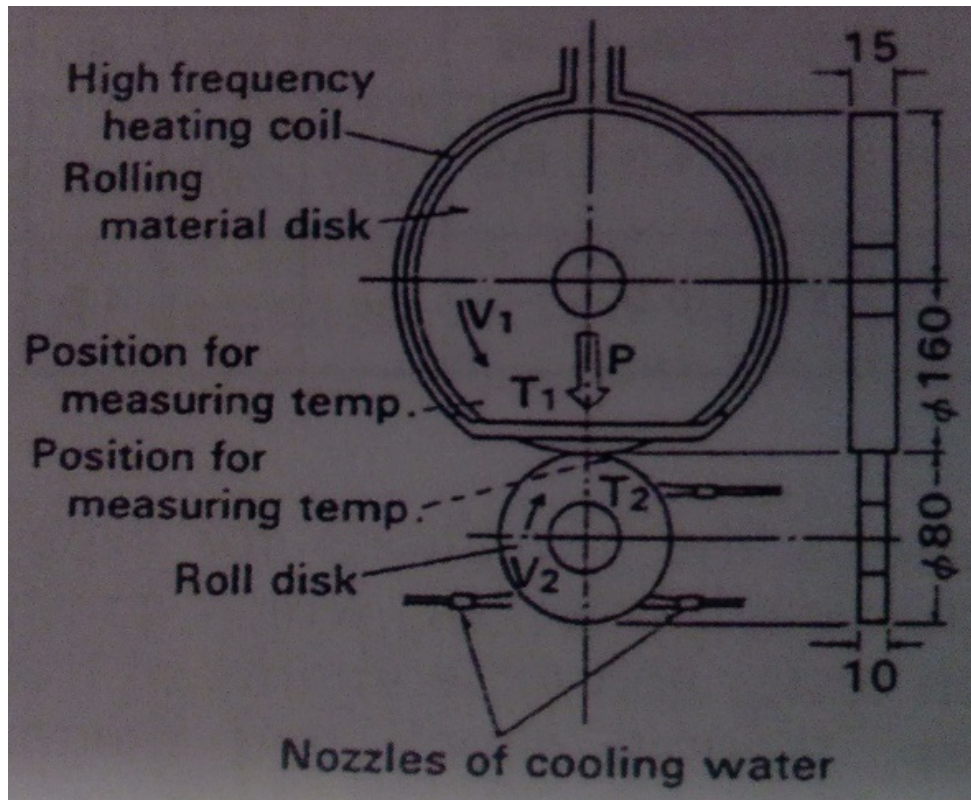


Figure 2-34: Hot wear testing two-disk device [15]

Testing procedure:

Setup parameters	Hot wear test method	Adhesion resistance test method
Rolling speed	2,9 m/s	0,21 m/s
Slippage	11 %	Until adhesion occurs
Testing temperature	Hot strip disk: 850 °C Hot roll disk: 500 °C	Hot strip disk: 870 °C Hot roll disk: 500 °C
Rolling force	686 kN = 235 MPa Hertzian pressure	441 kN = 196 MPa Hertzian pressure
Sample geometry	Sample disk: $d_a = 80$ mm $b = 10$ mm Hot strip disk: $d_a = 160$ mm $b = 10$ mm	Sample disk: $d_a = 80$ mm $b = 10$ mm Hot strip disk: $d_a = 160$ mm $b = 10$ mm
Testing duration	10000 rotations	50 rotations

Table 2-35: Testing parameters

2.5.10 Mechanisms of Surface Deterioration of Roll for Hot Strip Rolling [16]

Another approach of Yamamoto's wear testing procedures was researched on to get more information about his experiments to measure wear. The same machinery as in **Figure 2-34** was used as was the S45C hot strip disk. This time the testing parameters were changed. [16]

Testing procedure:

Setup parameters	Values
Rolling speed	Hot roll disk: 700 rpm
Slippage	11 %
Testing temperature	Sample disk: 500 °C Hot strip disk: 900 °C
Rolling force	250 MPa Hertzian pressure
Sample geometry	Sample disk: $d_a = 80$ mm, $b = 10$ mm Hot strip disk: $d_a = 160$ mm, $b = 10$ mm
Testing duration	10010 rotations

Table 2-36: Testing parameter

2.5.11 Summary

Table 2-37 sums up all the researched information of the science papers to give a better overview of all the testing parameters. This makes a later comparison with ESW's requirements easier and should present a base for the wear measurement device since the necessary experience is missing. The different testing methods showed some similarities which will be pointed out:

Mechanical setup:

Many devices showed a two- or three-disk device with a hot roll, hot strip and/or a backup disk. The load or pressure is transmitted through the disks via various mechanisms. Different slippage parameters exist and form the base to simulate the rubbing during the forming process in a hot roll mill. The rotations of the disks were often defined independently with different rolling speeds of the torque engines. Setting up the tests with disks allows a continuous testing without running low on real strip coils because of their disk-shaped form.

Reference	Rolling speed	rpm	Testing temperature	Force/Pressure	Slippage	Testing duration
[5]	0,015 mm/s	X	700 – 850 °C	15 – 45 kN	X	X
[6]	0,09 – 0,19 m/s	45 - 90	700 – 850 °C	150 - 300 N	X	1st: 7 min, 2nd: 10 min, 3rd: 10 min
[7]	0,47 & 0,52 m/s	180 & 200	700 – 850 °C	300 N ~ 300 MPa	28%	3 x 60 min
[8]	0,3 m/s	130	850 °C	600 MPa	34%	12000 revolutions (92 min)
[9]	X	X	1250 °C	X	X	Method 1: 8 hours Method 2: Up to 7 trials (1 trial: 0,8 – 1,3 km)
[10]	0,25 & 0,5 m/s (sliding distance/s)	X	900 °C	200 – 400 N	X	X
[11]	1,05 & 0,05 m/s	X	700 °C	100 MPa	X	Wear test: 10000 cycles, Friction test: 60 s
[12]	X	X	X	X	X	X
[13]	2,9 & 0,21 m/s	X	Hot strip disk: 850 - 870 °C Hot roll disk: 500 °C	196 & 235 MPa	11%	Hot wear test: 10000 rotations, Adhesion resistance: 50 rotations
[14]	X	700	Sample disk: 500 °C Hot strip disk: 900 °C	250 MPa	11%	10000 rotations

Table 2-37: Summarization of testing parameters

Temperature setup:

The heat was often conducted with an induction heating system which heated up a hot strip disk. This was to simulate the metal strip that would be deformed by the hot rolls in production process. This heating method assured a fast and mostly homogenous heating which is complicated because of the disks movement. Alternatively, torching flames were also used to heat up the strip disks. Temperature was often measured with pyrometers. This is an easy and effective method because the heated disks are moving permanently which does not allow solutions like thermocouples.

Mass measuring:

Another similar method in measuring the wear was weighting the sample before, during and after the testing procedures. The only difference was the dependence of the mass loss (either to volume, to slipping distance, etc.). This method shows a rather easy way of measuring the wear of the hot roll samples.

Sample geometry:

Almost in every case the sample were formed like a disk. Due to this method, it is possible to continuously proceed the testing without any limits to the rolling distance. A smaller and easier setup was achieved with it and the Hertzian law could be applied very well with a cylinder-cylinder case (chapter **2.4.1**). The identification of the sample's mass loss is also easier to determine since a regular weighing machine (depending on the accurateness) could be used.

3 Concept and development of the wear testing procedure

3.1 Definition of the task

To find out the right setting for the wear measurement device a clear testing goal must be set, since there are no standardized wear testing methods. It is important to know what needs to be measured and how it can be achieved to get as close as possible to industrial hot rolling. As mentioned in the previous chapter a change of the sample's mass was often determined as was the change of volume. A second effective method is shown in the ISO 4649 standard. While the standard is setup to determine the abrasion resistance of rubber, it still shows that approaching the loss of volume is also a possibility. ISO 4649 defines abrasion resistance “[...] either as a relative volume loss compared to an abrasive sheet calibrated using a standard reference compound, or as an abrasion resistance index compared to a reference compound.” [17]

Both methods – the mass and volume loss – are good indicators to measure the wear of hot rolls. They are easy to determine using simple measuring methods and a quite accurate depending on the measuring equipment. It is necessary to mention that phenomena like corrosion and other microstructural destructive processes cannot be determined with these methods and must rather be analyzed in a metallographic approach to characterize the wear more accurately. Otherwise it is not possible to define to what extent the various wear modes like abrasion, adhesion, tribo-oxidation or surface fatigue wear are contributing to a different extend since all of them include a loss of mass or volume.

3.2 ESW's testing factors and comparison to the researched testing factors

Table 3-38 shows ESW's aimed testing factors which were defined on a meeting in Tenneck on the 11th March 2016:

Setup parameters	Values
Temperature	900 - 1000 °C
Speed of rolls	100 rpm
Number of rolls	2 - 3
Slippage	0 - 7 %
Rolling force/pressure	1000 MPa Hertzian pressure
Testing duration	8 h (1 work day)
Sample roll diameters	$d_a = 40 - 50$ mm, $b = 10$ mm

Table 3-38: Testing parameters ESW

In **Table 3-39** a comparison of the testing parameters between ESW's aimed setup, literature research and Prof. M. Pellizzari's approach are listed:

Setup parameters	ESW	Literature	Pellizzari's approach
Temperature	900 - 1000 °C	500 - 1250 °C	700 °C
Speed of rolls	100 rpm	45 – 700 rpm	200 rpm
Number of rolls	2 - 3	2 - 3	2
Slippage	0 - 7 %	11 – 34 %	7 %
Rolling force/pressure	1000 MPa Hertzian pressure	15 – 45 kN or 100 – 600 MPa	1000 MPa Hertzian pressure
Testing duration	8 h (1 work day)	Up to 8 hours	8 h (1 work day)
Sample roll diameters ($d_a = \dots$, $b = \dots$)	$d_a = 40 - 50$ mm, $b = 10$ mm	$d_a = 40 - 120$ mm, $b = 10 - 30$ mm	$d_a = 50$ mm, $b = 10$ mm

Table 3-39: Testing parameters - comparison

Due to the lack of experience in the wear measurement of hot rolls, a meeting with Prof. Pellizzari was arranged so it was possible to see his adapted Amsler tribometer testing rig first hand and get further information about his testing results. His research showed a good representation of

the actual industrial process which is why his testing rig will serve as a mechanical model to the newly developed wear measurement device. Testing factors like the temperature or the speed of rolls will also be based on his testing method.

3.3 Concept of the hot roll measurement device and testing procedure

3.3.1 Concept drawing of the testing device

Figure 3-40 shows a hand drawing of the measurement device. It is based on the testing method described in chapter 2.5.3. It consists of two tables: each table has a power unit to create the necessary torque which is then led through a coupling to a shaft. The shaft is set in a double bearing system to create a stable stiffness. At the end of the shaft a disk can be mounted on and

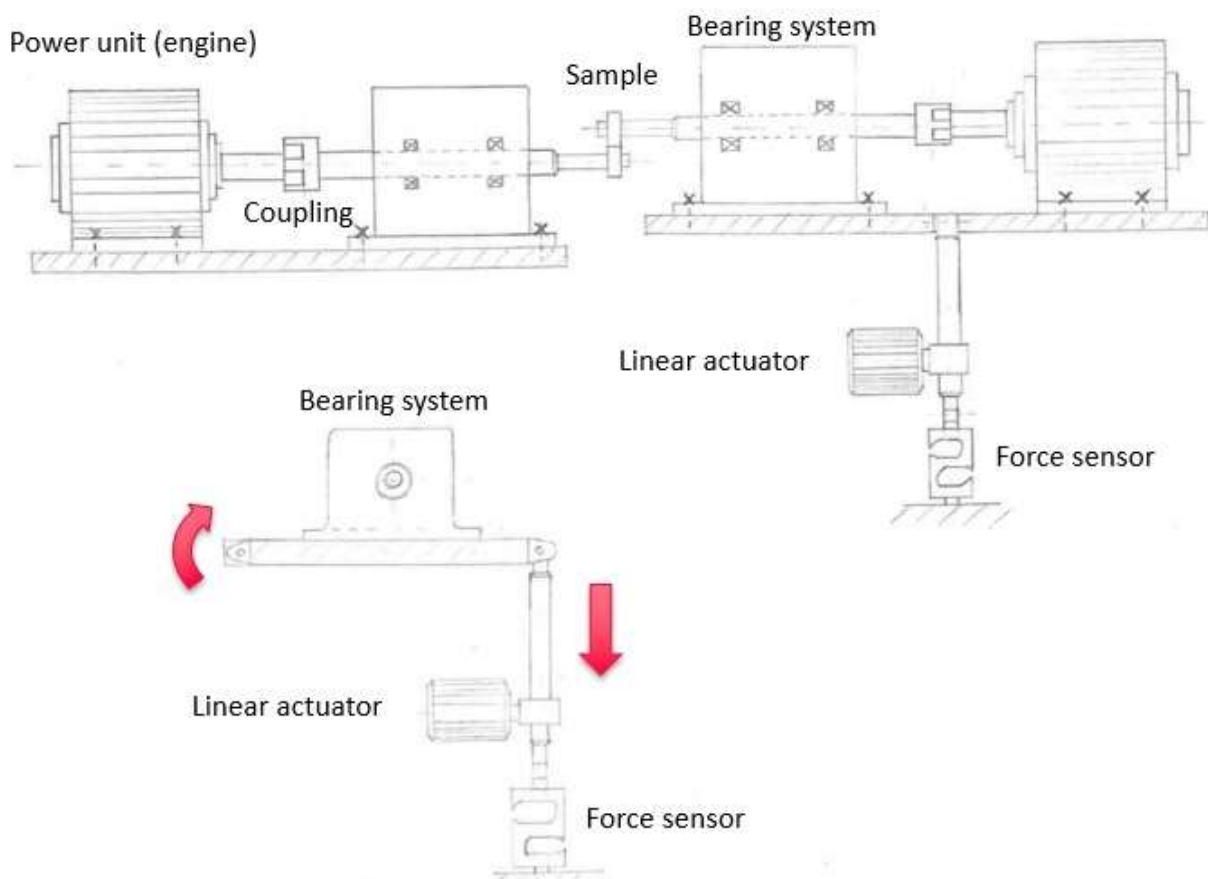


Figure 3-40: Concept drawing of the measurement device

fixed with a screw nut. The left side of the testing rig is stiff and does not move. The right table can be folded with a linear actuator on which end a S-force sensor is attached to measure the force. By folding the right table down the upper disk (hot rolling sample) is pulled down to the

bottom disk (hot mill strip disk) and thus applying the pressure on it. The actuator is connected to the table with a joint while the attached Z-force sensor is connected to a base with a joint. With this setting a radial adaption of the linear actuator is possible while the force sensor will always stay on the same force line (parallel) as the actuator.

3.3.2 Testing procedure

The wear testing will be proposed in the following way:

1. A disk-shaped sample of a hot roll ($d_a = 50 \text{ mm}$, $d_i = 20 \text{ mm}$, $b = 10 \text{ mm}$) is to be prepared (**Figure 3-41**).

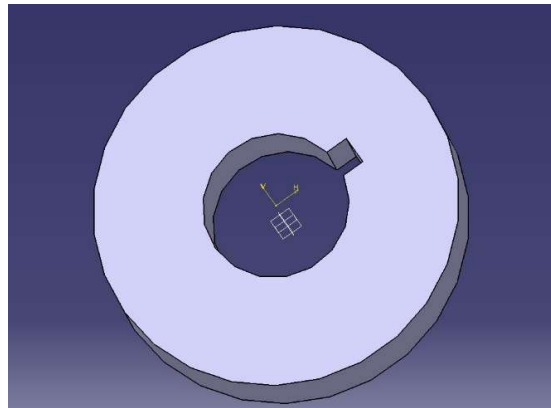


Figure 3-41: Sketch of hot roll sample and strip disk

The sample is then weighed and the outer diameter as well as the thickness are also measured 3 times using a caliper. It is recommended to measure the outer diameter with a 120° angle shifting and then calculating the mean.

2. The hot roll sample and strip mill disk (C40 steel, $d_a = 50 \text{ mm}$, $d_i = 20 \text{ mm}$, $b = 10 \text{ mm}$) are to be fixed on the shaft and then heated up by an induction heating system (by now there is no real data on the induction heating system of the TU Graz so it cannot be determined how long it will take to get a homogenous temperature profile which will be observed via pyrometers).

3. The testing procedure with the defined Hertzian stress, torque, slippage, temperature and testing time is to be started.

4. After the first testing period and cooling down of the sample, the diameter and thickness are measured again so is the weight. Both are plotted against the distance or revolutions covered during the testing period.

5. Repeat this procedure as many times as needed.

3.4 Calculations

3.4.1 Hertzian pressure

As the Hertzian pressure needs to be calculated into the applied force for a 10 mm thick disk, equation (18) is used for the case of two parallel cylinders:

$$p_0 = \frac{2F}{\pi L a} \approx \sqrt{\frac{EF}{\pi LR}} \quad (18)$$

$$F = \frac{p_0^2 \pi LR}{E} \quad (19)$$

With

$$P_0 = 1000 \text{ MPa}$$

$$L = 10 \text{ mm}$$

$$R = 50 \text{ mm}$$

Since the properties of the hot roll sample are not known, for the simple case of two similar steel disks the calculation will set up:

$$E_{\text{steel}} = 210.000 \text{ N/mm}^2$$

Also because of the two disks being setup similar and are now assumed to be made of steel one can change (15) to

$$\frac{1}{E} = \frac{1-\vartheta^2}{E} \quad (20)$$

setting the Poisson number ϑ for steel:

$$\vartheta = 0,30 \text{ (p.C4) [3]}$$

Inserting (20) into (19) one gets for the force F :

$$F = \frac{p_0^2 \pi LR (1 - \vartheta^2)}{E} = 6,8 \text{ kN}$$

For the hot roll sample will have a different E-modulus and a different Poisson number, (15) has to be recalculated by the operator if a correct conversion of F and p_0 is needed.

3.4.2 Torque

In order to know how much torque for a pressure force of 6,8 kN is needed from the engines that spin the disks, equation (10) is used. For the case of a lubricated rolling friction with a steel on steel disk procedure:

$$R = \mu N = 680 \text{ N}$$

$$\mu = 0,1 \text{ (p. B15) [3]}$$

$$F = N = 6,8 \text{ kN}$$

Now we multiply R with the radius of the disk ($r = 25 \text{ mm}$) and get for the torque $M = 17 \text{ Nm}$.

3.5 Mechanical parts

This chapter describes the properties of the mechanical parts which were used based on the testing properties. It needs to be mentioned that some parts and setups were chosen due to the experience of the part's seller. Since the hot roll testing parameters are not yet defined entirely and some changes may appear during the first testing rounds, all parts were chosen in a way so that the needed parameters could always be risen slightly higher.

3.5.1 Power unit

The power unit for the disks are two sync engines with a terminal pair of 3 (model 8LSA73) build by B&R Automation. Sync engines are known to run more stable which is why they are chosen. The torque runs up to 26 Nm and have a rotational speed with 3000 rpm. Besides changing the torque and rpm to any needed value the advantage of this power unit series is that a slippage can be adjusted due a power touch panel, thus no gear system is needed. A servo amplifier is able to change the rpm of each power unit and makes is possible to achieve a negative slippage (counter rotation). **Figure 3-42** shows the setup of the power unit system.

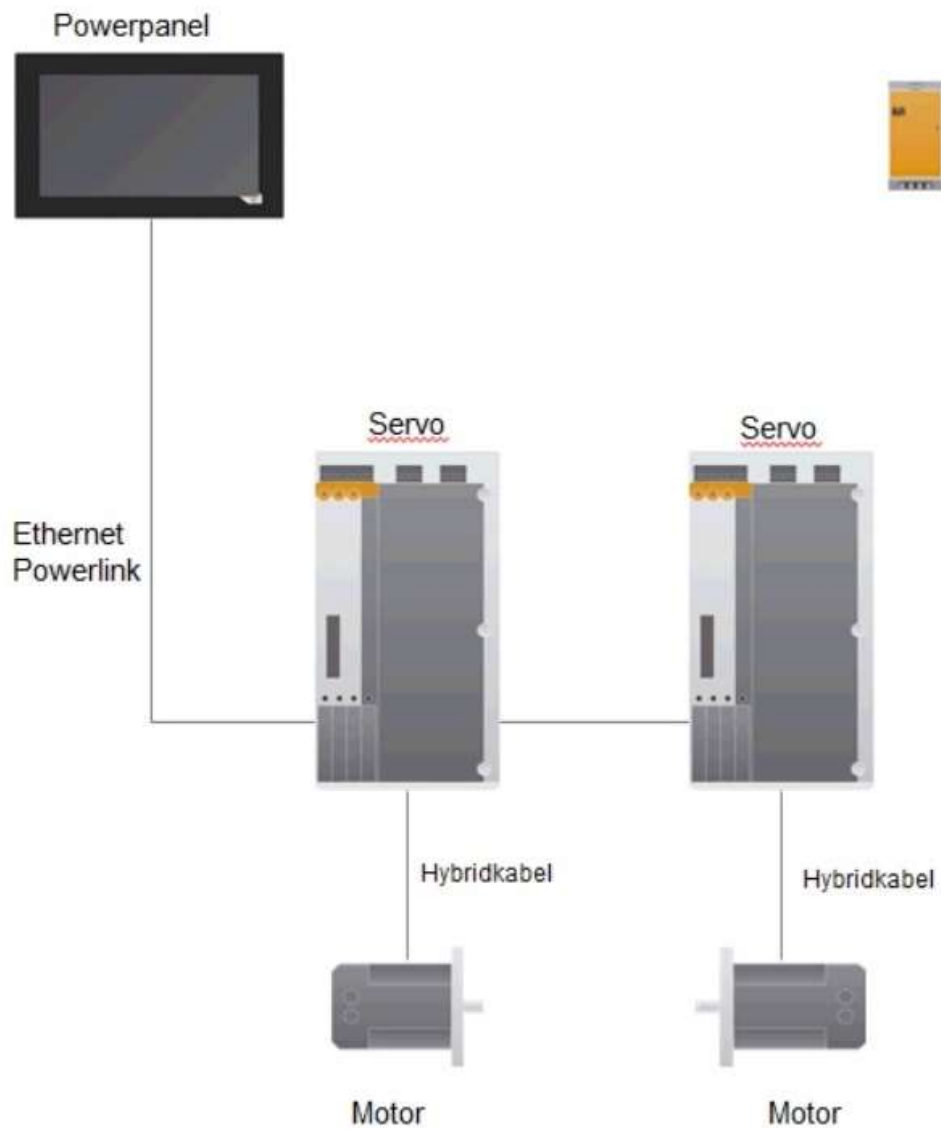
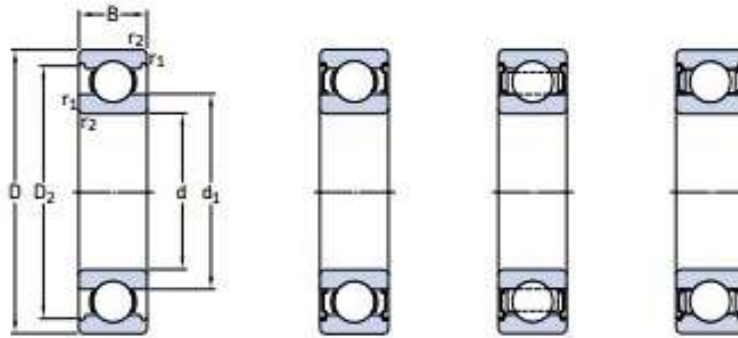


Figure 3-42: Power unit setup for the 8LSA73 series from B&R Automation [18]

3.5.2 Bearing system

Since a regular bearing system cannot be used in the wear measurement device because of the high temperature of the hot roll disk, SKF [19] offers a solution where a high temperature double bearing system can be used. The bearings can have a basic load of 7,28 kN and are dynamic (which is needed due the possible vibrations of the samples change of surface during the wear procedure). The accepted rotational speed is set to 230 rpm. Though the official data sets the service temperature of the bearings to a limited 350 °C, SKF assured that due self-cooling effects the bearings will perform as needed. Since Prof. Pellizzari's device didn't have special bearings it is presumed that this selection will be sufficient. **Figure 3-43** shows the chosen deep groove bearings.

15B.1 Single row deep groove ball bearings for extreme temperatures
d 10 – 65 mm



Dimensions						Basic static load rating	Limiting speed	Mass	Designation
d	D	B	d ₁	D ₂	r _{1,2} min.	C ₀			
mm						kN	r/min	kg	-
10	35	11	17,5	28,7	0,6	3,4	400	0,053	6300-ZZ/VA201
12	32	10	18,4	27,4	0,6	3,1	400	0,037	6201/VA201
	32	10	18,4	27,4	0,6	3,1	400	0,037	6201-ZZ/VA201
	32	10	18,4	27,4	0,6	3,1	400	0,037	6201-ZZ/VA228
15	35	11	21,7	30,4	0,6	3,75	360	0,045	6202/VA201
	35	11	21,7	30,4	0,6	3,75	360	0,045	6202-ZZ/VA201
	35	11	21,7	30,4	0,6	3,75	360	0,045	6202-ZZ/VA228
17	35	10	23	31,2	0,3	3,25	340	0,038	6003/VA201
	35	10	23	31,2	0,3	3,25	340	0,038	6003-ZZ/VA201
	35	10	23	31,2	0,3	3,25	170	0,038	6003-ZZ/VA208
20	40	12	24,5	35	0,6	4,75	310	0,065	6203/VA201
	40	12	24,5	35	0,6	4,75	310	0,065	6203-ZZ/VA201
	40	12	24,5	35	0,6	4,75	310	0,065	6203-ZZ/VA228
	47	14	26,5	39,6	1	6,55	280	0,11	6303/VA201
	47	14	26,5	39,6	1	6,55	280	0,11	6303-ZZ/VA228
	47	14	28,8	40,6	1	6,55	260	0,031	6204-ZZ/VA201
25	42	12	27,2	37,2	0,6	5	290	0,067	6004/VA201
	42	12	27,2	37,2	0,6	5	140	0,067	6004-ZZ/VA208
	47	14	28,8	40,6	1	6,55	260	0,031	6204/VA201
	47	14	28,8	40,6	1	6,55	260	0,031	6204-ZZ/VA201
	47	14	28,8	40,6	1	6,55	260	0,031	6204-ZZ/VA228
	52	15	30,3	44,8	1,1	7,8	250	0,14	6304/VA201
30	52	15	30,3	44,8	1,1	7,8	250	0,14	6304-ZZ/VA201
	52	15	30,3	44,8	1,1	7,8	250	0,14	6304-ZZ/VA228
	47	12	32	42,2	0,6	6,55	250	0,078	6005/VA201
	47	12	32	42,2	0,6	6,55	250	0,078	6005-ZZ/VA201
	47	12	32	42,2	0,6	6,55	120	0,078	6005-ZZ/VA208
	52	15	34,3	46,3	1	7,8	230	0,13	6205/VA201
35	52	15	34,3	46,3	1	7,8	230	0,13	6205-ZZ/VA201
	52	15	34,3	46,3	1	7,8	230	0,13	6205-ZZ/VA228
	62	17	36,6	52,7	1,1	11,6	200	0,23	6305/VA201
	62	17	36,6	52,7	1,1	11,6	200	0,23	6305-ZZ/VA228
	62	17	36,6	52,7	1,1	11,6	200	0,23	6305-ZZ/VA208
	62	17	36,6	52,7	1,1	11,6	200	0,23	6305-ZZ/VA228

Figure 3-43: High temperature performance bearings of SKF [19]

3.5.3 Force sensor

To measure the force which the linear actuator applies onto the disks, an S-type force sensor from tectis is chosen. The model F2211 (**Figure 3-44**) can measure up to 10 or 20 kN depending on the version and is suited for push and pull forces. An online and digital measuring of the disk force is enabled due to a digital output and is also compatible with conventional software such as LabVIEW. Two tap holes make it possible to install the sensor to the base and the linear actuator. Since a load of 6,8 kN is applied onto the sample the 20 kN version is still recommended because of experience: A “stronger” force sensor usually has a longer life time since it is not used close to its limits.



Figure 3-44: S-type force sensor F2211 [20]

3.5.4 Screw linear actuator

A screw linear actuator makes it possible to apply the testing force with a vertical screw movement. ACME’s model CLA 28 can apply a pull-push force of 10 kN. The stroke length varies from 200 to 800 mm. An advantage of this screw linear actuator is the changeable head which makes it possible to attach a joint onto it which connects it with the table where the sample holding system is mounted on. A mechanical overload protection also serves as a safety method to avoid possible damage to the system.

3.5.5 Clutch/coupling

A tolerance-free coupling arrangement connects the shaft of the power unit with the testing shaft. Since the power units produce a torque of 26 Nm, a claw coupling with a durable torsion $T_{KN} = 26 \text{ Nm}$ was chosen to assure a stable torque transfer: ROTEX GS – Size 19. [21]

3.5.6 Induction heating

The heating of the hot roll sample is done by an induction heating system. Since this method allows a fast and relatively homogenous heating for moving parts, the use of such a system is of great advantage. However, due to the high price of over 30.000 €, the TU Graz offered using their own home device as a solution for ESW (**Figure 3-45**). Since no further information about the heating system and plans were available at that time, the adaption of the induction system is to be shifted to the second part of the project, where an adequate setup can be arranged and the proper heating coil can be determined.



Figure 3-45: Induction heating system of the TU Graz

4 Results

4.1 Constructed device

The device will be a two disk-on-disk device which consists of a hot roll sample and a hot strip sample (for example C40 steel). This method allows a continuous, quick and cost-efficient method to simulate the wear of the hot roll samples since no strip coils or big hot roll rigs are required and is very compact in comparison. Base on the Hertzian law it is possible to apply the necessary force of 6,8 kN on the two-cylinder model. The speed of the rolls (200 rpm) and the slippage are also adaptable because of the servo-controlled power unit system which always allows a change of the testing parameters if needed. With the screw linear actuator attached to the table folding system, the pressure/force can be applied onto the sample by pulling the upper part of the table down. This can also be measured by the S-type force sensor beneath the actuator which preferably has the range to 20 kN. A modified bearing system is to be used with high temperature bearings due to the induction heating of the sample. A short shaft also guarantees stiffness of the system to assure, that the surfaces of the testing rolls are staying parallel to each other. **Figure 4-46** shows the concept drawing with the exclusive designed table folding system. The hot roll wear measurement device was constructed on designed via Catia V5. The appendix includes the drawings for the device as well as a parts list. The induction heating system is excluded as mentioned in **3.5.6** since no clear data was available on the system.

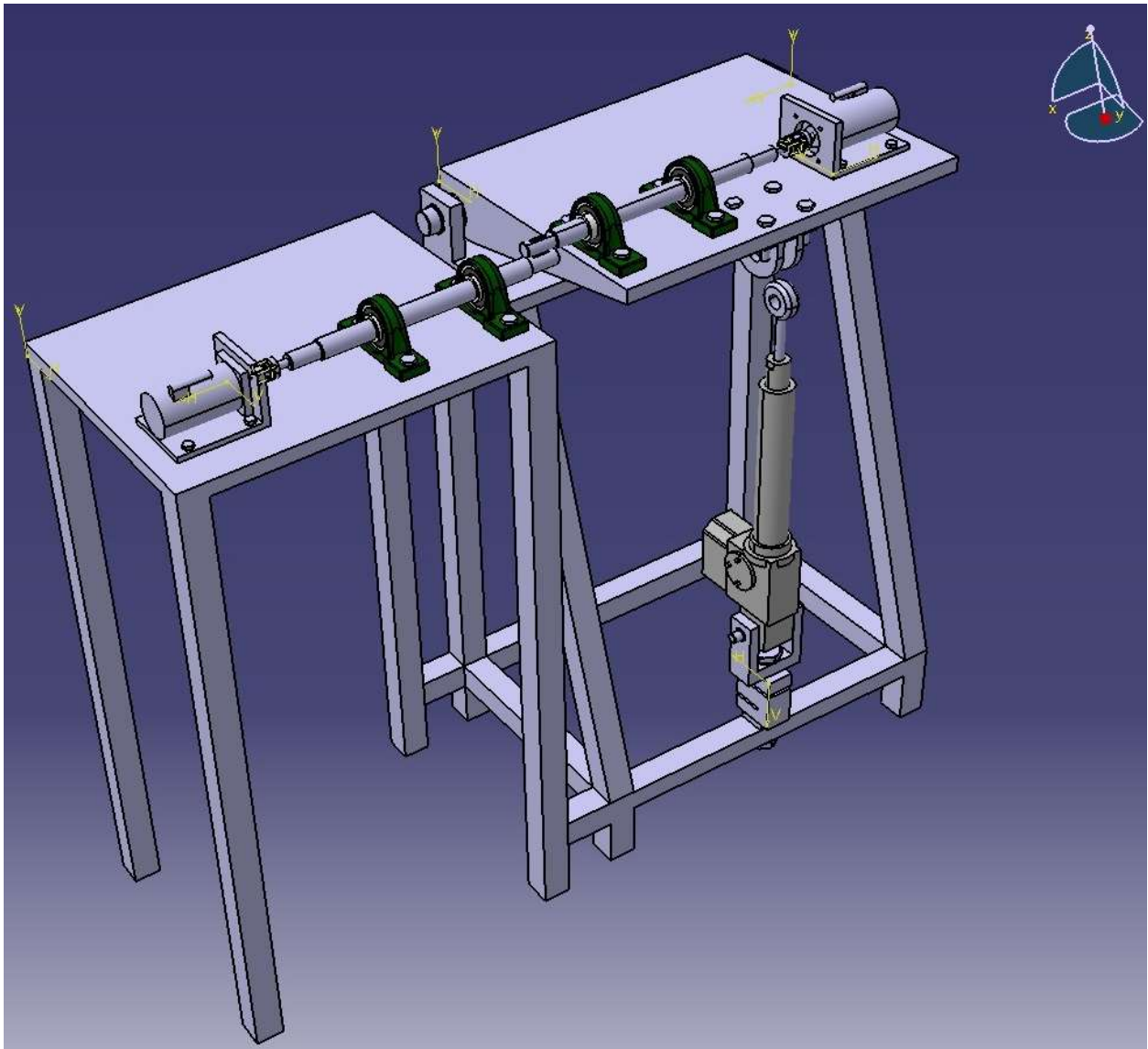


Figure 4-46: Concept of the wear measurement device

4.2 Cost

Since the financial aspect was a deciding factor for the concept, a cost-benefit solution had to be found. Measuring devices can easily cost several hundred thousand Euros. One solution to lower the costs, is the possibility to build some mechanical parts at the workshop of the university. CNC machines are available, such as an induction heating system which was originally planned to be purchased for around 30.000 Euros from the company iew GmbH. **Table 4-46** shows an overview of the expected costs. At this point it needs to be mentioned that the exact costs cannot be determined since many parts are build in-house. All other expenses are based on offerings which were directly requested from the producer and to be found in the appendix or were looked up in their official catalogue.

Parts	Costs
Power units (8LSA73)	3400,00 €
Bearing system (SKF High temperature bearing system)	600,00 €
Force sensor (F2211)	300,00 – 400,00 €
Screw Linear Actuator (CLA 28)	700,00 €
Clutch/Coupling (Rotex GS)	100,00 €
Screws, table, induction coil, other parts	No information available (In-house production)

Table 4-47: Summary of the costs

It is assumed that the final costs will be around 10.000 – 12.000 Euros. The prices only include the machine parts. Additionally, the charge may rise due guarantee, service, installation or startup expenses that can be optionally purchased.

5 Discussion of concept

The development of the wear measurement device for hot rolls required a careful gathering of information for the approach since no standardized system exists. The first step was to understand the physical and mechanical phenomena that occur during the forming process of hot rolling. Since tribology is one of the most important discipline in the rolling process, several mechanisms of wear needed to be analyzed in order to define a common factor to define wear: The loss of mass or volume. Naturally, wear includes many other different factors, but a generalization had to be made. Another necessary step is to understand the contact mechanical process during hot rolling and Hertzian's law. It sets the base for the concept as a possibility to calculate the pressure p_0 or force F between two cylindrical objects which operate under a mixed slide-rolling friction effect. Since this two-cylinder case goes very well with the two-disk testing model, the device is designed like this. The calculated force of 6,8 kN can be put into effect as well as the needed torque by purchasable devices. An undesired factor are the bearings in terms of the temperature. Since the set testing temperature is set to 700 °C, it is not known to what extend the bearings will be a critical factor in the device. Based on Prof. Pellizzari's device which includes regular bearings it should be sufficient. The testing procedure is set in several testing cycles where after each testing round the loss of mass and volume is determined based under the set definition of wear. A further analysis of the samples is necessary, since the main wear mode cannot be determined with this method.

Compared to other tribological devices in the industry where their financial value can easily reach multiple 6-digit numbers, the expected costs of around 12.000 Euros are very low cost. This is possible due in-house building of several parts as of the induction heating system which is the most expensive part of the device. Additionally, a unique heating coil has to be made for the sample, since no standard coils exist.

6 Conclusion

The goal of the project is to develop and construct a measurement device to determine the wear of hot rolls for the company ESW. Since the research and development of hot rolls represent a complicated process due their complex chemical composition, tribological behaviour and mechanical properties, the determination of the quality of hot rolls is very hard. The approach of creating a device and technique to measure the wear shows a difficult task, because of the many physical processes that take place. To find a solution, an engineering approach is generally to simplify the problem. By comparing different methods, it was possible to find a concept that covers the mass and volume loss of the test specimen as well as the mechanical testing method. By simulating the rotational and slipping movement of the rolling process, the tribological occurrences could have been copied to an extent to produce a similar tribological effect on the test samples. Since the testing parameters vary with different testing methods, the parts for the device have been chosen and designed, so different temperatures, rolling speed and forces can be applied. A testing procedure has also been added, where several test-cycles allow a step-by-step measuring of the samples. Also, keeping the financial aspect in mind, this device shows its advantage of being very low cost. Since testing devices are very expensive due to the maker's patents, this device represents a pricey approach to develop a measurement machine for wear.

7 Suggestions and outlook

Since wear represents a complex tribological behaviour, it takes several steps to build a full reliable simulation device. The outlook for this project will show the next necessary steps to be done as well as suggestions to develop a more realistic and safer simulation device.

1. The first step will be the building of the device. Since it is possible to produce several parts in the workshop of the university, it must be decided what has to be purchased and what has to be built. A CNC machine allows creating parts as shafts, pins, etc. Since this device is a concept it is still possible that parts of the machine might be changed due either production difficulties, change of design due recommendations with the production department or other occasions. It is very common that changes to the original design are made because of those reasons.
2. Test runs need to be made. Before starting the testing, it needs to be assured that the device works properly. Additionally, a calibration process has also to be done - no data has any value if the testing device is simulating the hot rolling process wrong. By doing this the functionality can be confirmed.
3. Data gathering of experimental test runs are an important step to check if testing technique makes sense. By running various simulations with different samples and parameters it is possible to compare them and set the testing conditions. By using the design of experiment one can also set the base of the information that is gathered in terms of the testing conditions.
4. Once the simulation device is working properly and is brought into service, it is still possible to add additional features to get a higher quality of the simulation, handling and safety. Suggestions are:

Controlling software implementation

By adding a custom-made software implementation (for example LabVIEW) to the system, it is possible to control the whole process on one device. Temperature, rolling speed, pressure and testing time can be set up by one program to assure a common source of incoming data.

This may help the handling of the testing as well as an easy method of controlling to assure a more standardized testing.

Atmospheric coverage

A cover around the samples makes it possible to apply atmospheric testing procedures. Implementing this feature allows to measure the wear without the influence of tribo-oxidation if argon or other inert gasses are used. This allows a better differentiation of the wear processes very similar to the Gleeble which also has a gas cover implemented. An additional advantage is the safety aspect: Since the hot samples are covered, the operator is not able to touch the sample area and get harmed.

List of references

- [1] <http://www.massivumformung.de/1/industry/history-of-metal-forming/>
- [2] Fritz, A. H., & Schulze, G. (2007). *Fertigungstechnik*. Berlin: Springer-Verlag, 8.Auflage.
- [3] K.-H. Grote & J. Feldhusen (2007). *Dubbel – Taschenbuch für den Maschinenbau*. Berlin: Springer-Verlag, 22. Auflage.
- [4] Dietmar Gross, Werner Hauger, Jörg Schröder, Wolfgang A. Wall, (2008). *Technische Mechanik – Band 1: Statik*. Berlin: Springer-Verlag, 10. Auflage
- [5] Valentin L. Popov (2015). *Kontaktmechanik und Reibung – Von der Nanotribologie bis zu Erdbebendynamik*. Springer-Verlag, 3. Auflage
- [6] Anh Kiet Tieu, Qiang Zhu, Hangtao Zhu, Cheng Lu (2011). *An investigation into the tribological behaviour of a work roll material at high temperature*. School of Mechanical, Materials and Mechatronics Engineering, University of Wollongong, Australia
- [7] J.J. Fithpatrick and J.G. Lenard (2000). *The wear of tool steel rolls during hot rolling of low carbon steels*. Department of Mechanical Engineering, University of Waterloo
- [8] M. Pellizzari, D. Cescato, M.G. De Flora (2009). *Hot friction and wear behaviour of high speed steel and high chromium iron for rolls*. Department of Materials Engineering and Industrial Technologies, University of Trento
- [9] M Pellizzari, A. Molinari, G. Straffelini (2004). *Tribological behaviour of hot rolling rolls*. Department of Materials Engineering and Industrial Technologies, University of Trento
- [10] Joon Wook Park, Hui Choon Lee, Sunghak Lee (1999). *Composition, Microstructure, Hardness, and Wear Properties of High-Speed Steel Rolls*. Roll Manufacturing Division, Kangwon Industries
- [11] G. Walmag, J. Malbrancke, J. Sychterz, A. Brown, S. Mul, E. van den Elzen (not dated). *Laboratory and pilot mill scale evaluation methods for evaluating new work roll grade incorporating NDT methods*. Centre de Recherches Métallurgiques, Liège; Union Electric Steel UK Limited, Gateshead; Lismar Engineering B.V., Ouderkerk aan de Amstel

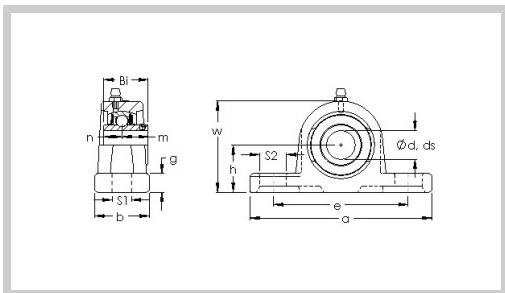
- [12] G. Savage, R. Boelen, A. Horti, H. Morikawa, Y. Tsukimoto (1996). *Hot wear testing of rollalloys*. Broken Hill Proprietary Co. Ltd., Kubota Corporation
- [13] Kunio Goto, Yukio Matsuda, Kohichi Sakamoto, Yoshihito Sugimoto (1992). *Basic Characteristics and Microstructure of High-carbon High Speed Steel Rolls for Hot Rolling Mill*. Iron & Steel Research Laboratories, Sumitomo Metal Industries Ltd.
- [14] Gisèle Walmag, Sébastien Flament, Jurgen Malbrancke, Geneviève Moreas, Mario Sinnaeve (not dated). *Development of new materials based on on-site and laboratory evaluation methods for understanding work roll surface degradation*. CRM Group (Belgium)
- [15] Hiroyasu Yamamoto, Shigeru Uchida, Syoichi Araya, Koue Nakajima, Mitsuo Hashimoto, Kazuo Kimura (not dated). *Characteristics of high-speed tool steel as material of work roll in hot rolling*. Technical Development Bureau & Plant and Machinery Division, Nippon Steel
- [16] Osamu KATO, Hiroyasu Yamamoto, Matsuo Ataka, Koe Nakajima (1992). *Mechanisms of Surface Deterioration of Roll for Hot Strip Rolling*. Mechanical Working Process & Process Technology Research Laboratories, Nippon Steel
- [17] Standard ISO 4649:2010-09. *Rubber, vulcanized or thermoplastic – Determination of abrasion resistance using a rotating cylindrical drum device*. Austrian Standards Institute
- [18] Thomas Dicker (28.11.2016). *Angebot Entwicklung und Konstruktion einer Verschleißprüfmaschine (Angebotsnummer A100.16.1712 V001)*. B&R Automation Eggelsberg
- [19] <http://www.skf.com/binary/77-121486/SKF-rolling-bearings-catalogue.pdf> (p. 1178)
- [20] https://www.tecsis.de/fileadmin/Content/tecsis/2_Files/1_Force/H_Tension-Compression_Force_Transducers/dd921.pdf
- [21] <https://www.ktr.com/eMag/Antriebstechnik2017/pubData/mobile/index.htm#/120/>

List of figures

- Figure 2-1:** Classification of forming according to DIN 8582
- Figure 2-2:** Classification of rolling according to DIN 8583
- Figure 2-3:** Unicell structure of metals: Body-centered cubic (left), face-centered cubic (center), hexagonal closed-packed (right)
- Figure 2-4:** Illustration of duo, trio or quarto rolling systems
- Figure 2-5:** Parameters in longitudinal rolling with raw material between the rolls
- Figure 2-6:** Velocity of the deformed metal sheet during forming process
- Figure 2-7:** Vertical rolling force
- Figure 2-8:** Slide friction and rolling friction
- Figure 2-9:** Abrasive wear – two body (left), three body (right)
http://www.substech.com/dokuwiki/doku.php?id=mechanisms_of_wear
- Figure 2-10:** Adhesive wear of two surfaces
http://www.substech.com/dokuwiki/doku.php?id=mechanisms_of_wear
- Figure 2-11:** Surface fatigue wear
http://www.substech.com/dokuwiki/doku.php?id=mechanisms_of_wear
- Figure 2-12:** Inelastic ball entering an elastic room
- Figure 2-13:** Two cylinders touching each other with parallel axes
- Figure 2-14:** Illustration of mini two-high rolling mill
- Table 2-15:** Testing setup parameters
- Figure 2-16:** Stanat laboratory rolling mill
<http://www.introllingmills.com/gallery/view/3>
- Figure 2-17:** Illustration of the testing method
- Table 2-18:** Testing parameters
- Figure 2-19:** Amsler Tribometer http://www.hefusa.net/tribology_testing/tribology_resources.html
- Figure 2-20:** Setting of the hot rolling wear testing procedure
- Table 2-21:** Testing parameters
- Figure 2-22:** Setting of the wear test
- Figure 2-23:** Geometric description of the wear disk
- Table 2-24:** Testing parameters

- Figure 2-25:** Setup of the hot rolling simulation
- Figure 2-26:** “Insert sample” work roll for six samples
- Table 2-27:** Testing parameters
- Figure 2-28:** BHP testing rig
- Table 2-29:** Testing parameters
- Figure 2-30:** Wear test setting (left) and friction test setting (right)
- Table 2-31:** Testing parameters
- Figure 2-32:** Two-disk hot strip testing setup
- Figure 2-33:** Three-disk back-up roll testing setup
- Figure 2-34:** Hot wear testing two-disk device
- Table 2-35:** Testing parameters
- Table 2-36:** Testing parameter
- Table 2-37:** Summarization of testing parameters
- Table 3-38:** Testing parameters ESW
- Table 3-39:** Testing parameters - comparison
- Figure 3-40:** Concept drawing of the measurement device
- Figure 3-41:** Sketch of hot roll sample and strip disk
- Figure 3-42:** Power unit setup for the 8LSA73 series from B&R Automation
- Figure 3-43:** High temperature performance bearings of SKF
- Figure 3-44:** S-type force sensor F2211
- Figure 3-45:** Induction heating system of the TU Graz
- Figure 4-46:** Concept of the wear measurement device
- Table 4-47:** Summary of the costs

Appendix



Part Number: UCP205
Metric Series Two Bolt
Pillow Block



Product Details

Specifications

Bearing Type	Extended inner race with set screws	
Dynamic Load Rating (Cr)	14,022	N
Static Load Rating (Cor)	7,843	N
Shaft Dia. (Fw)	25.000	mm
Shaft Height (h)	36.500	mm
Housing Width (b)	38.000	mm
Mounting Hole Center-to-Center (e)	105.000	mm
Housing Length (a)	140.000	mm
Mounting Slot Length (S2)	19.000	mm
Mounting Slot Width (S1)	13.000	mm
Housing Base Thickness (g)	13.000	mm
Housing Height (w)	71.000	mm
Bearing Inner Race Width (Bi)	34.000	mm
Bearing Inner Race Width - Short Side (n)	14.300	mm
Bearing Inner Race Width - Extended Side (m)	19.700	mm
Mounting Bolt Size	10.000	mm
Bearing Number	UCP 205	
Housing Number	P 205	
Shaft Dia., Nominal (d)	25.000	mm
Weight (g)	816.00	grams
Material	Cast iron housing, chrome steel bearing	

* Also available with eccentric locking collar.

* Medium Duty, Heavy Duty and other available types are described in the Bearing Types information.

* Various seal options and plated housing options are described in the Nomenclature and Bearing Types information.

Value Beyond the Part™

All information in this catalog has been thoroughly checked for accuracy. However, AST Bearings assumes no liability for possible errors or omissions. All dimensions and specifications are subject to change without notice.

HEADQUARTERS:
115 Main Road
Montville, NJ 07045
(800) 526-1250

WEST COAST OFFICE:
3740 Prospect Ave
Yorba Linda, CA 92886
(800) 227-8786

email:
inquiry@astbearings.com

Engineering Consulting & Design
Bearing Applications Engineering
Quality Assurance Inspection &
Verification

Bearing Failure Analysis
Custom Packaging
Bearing Lubrication Services



3 Stromversorgungen

3.1 B&R-Hutschienennetzteil

Summe **netto 63,36 €**

Stückliste

Pos.	Menge	Bezeichnung	Rabatt	LP Einzel	LP Gesamt
3.1.1	1 Stück	OPS1050.1 24 VDC Netzteil, 1-phasig, 5 A, Eingang 100 bis 240 VAC, Wide Range, Hutschienenmontage	40,00 %	105,60 €	105,60 €



2 Antriebstechnik

2.1 B&R-ACOPOS

Summe **netto 2.717,40 €**

Stückliste

Pos.	Menge	Bezeichnung	Rabatt	LP Einzel	LP Gesamt
2.1.1	1 Stück	8V1180.00-2 ACOPOS Servoverstärker, 3x 400-480 V, 19 A, 9 kW, Netzfilter, Bremswiderstand, Zwischenkreisnetzteil und elektronische sichere Wiederanlaufsperr integriert	60,00 %	2.377,50 €	2.377,50 €
2.1.2	1 Stück	8AC126.60-1 ACOPOS Einsteckmodul, EnDat 2.2 Geber Interface	60,00 %	217,50 €	217,50 €
2.1.3	1 Stück	8LSA73.DA030S000-3 Synchron-Motor; Polpaarzahl: 3 Paar; Nenn Drehzahl: 3.000 min ⁻¹ Stillstandsmoment: 26,000 Nm; ohne Bremsen; glatte Welle; Stecker gewinkelt (drehbar) Einkabellösung; Zentrierdurchmesser 180 mm; Passung j6 selbstgekühlt, Bauform A; Schutzklasse IP64; ohne Wellendichtring 560 VDC; Haltemoment der Bremse: 0,00 Nm; DA ind. 32Strich singlet. V2	0,00 %	1.672,50 €	1.672,50 €
2.1.4	1 Stück	X20CA0E61.00050 POWERLINK-Verbindungskabel, RJ45 auf RJ45, 0,5 m	60,00 %	17,25 €	17,25 €



1 Visualisieren und Bedienen

1.1 B&R-Powerpanel

Summe **netto 594,06 €**

Stückliste

Pos.	Menge	Bezeichnung	Rabatt	LP Einzel	LP Gesamt
1.1.1	1 Stück	4PPC70.101G-20B Power Panel C70, 10,1", analog resistiver Touch Screen, Intel ATOM 333 MHz komp., 256 MByte DDRAM, 32 kByte FRAM, 2 GByte Flash-Drive on board, 1 X2X Link Schnittstelle, 1 POWERLINK-Schnittstelle, 1 Ethernet-Schnittstelle 10BASE-T/100BASE-TX, 2 USB 2.0 Schnittstellen, Basisgerät ohne Optionsboard, Querformat, anthrazit-pinstripe	60,00 %	1.461,00 €	1.461,00 €
1.1.2	1 Stück	0TB6102.2110-01 Zubehör Feldklemme, 2-polig (3,81), Federzugklemme 1,5 mm ²	60,00 %	2,70 €	2,70 €
1.1.3	1 Stück	X20CA0E61.00200 POWERLINK-Verbindungskabel, RJ45 auf RJ45, 2 m	60,00 %	21,45 €	21,45 €



PREISÜBERSICHT

Position	Menge	Ausführung	Einzelpreis	Gesamtpreis
1		Visualisieren und Bedienen		
1.1	1	B&R-Powerpanel	594,06 €	594,06 €
2		Antriebstechnik		
2.1	1	B&R-ACOPOS	2.717,40 €	2.717,40 €
3		Stromversorgungen		
3.1	1	B&R-Hutschienennetzteil	63,36 €	63,36 €
		Gesamtsumme		3.374,82 €

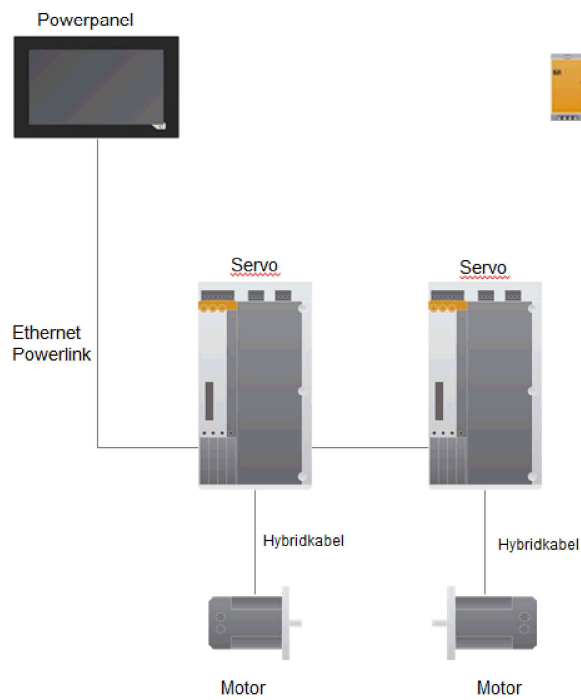


SYSTEMÜBERSICHT

TU Graz - EAM



Entwicklung und Konstruktion einer Verschleißprüfmaschine



Zug- /Druckkraftaufnehmer mit Innengewinde; S-Type

mit elektrischem Ausgang



Beschreibung

Das Einsatzgebiet dieses Kraftaufnehmers liegt sowohl in der Wägetechnik als auch in unzähligen Industrieapplikationen, wo hohe Genauigkeit, einfacher Einbau mit großer Auflagefläche und günstiger Preis eine entscheidende Rolle spielen.

Hier liefert dieser Kraftaufnehmer ideale Voraussetzungen in den Messbereichen von 0...2 kg bis 0...5000 kg und ist für Zug- und Druckkraftmessungen einsetzbar.

Dieser Kraftaufnehmer ist spritzwassergeschützt und arbeitet auch unter schwierigen Einsatzbedingungen zuverlässig.

Hinweis

Um Überlastung zu vermeiden, ist es vorteilhaft den Kraftaufnehmer während der Montage elektrisch anzuschließen und den Messwert zu überwachen.

Die Messkraft muss zentrisch und querkräftfrei eingeleitet werden.

Bei der Montage des Kraftaufnehmers sollte auf eine ebene Auflagefläche geachtet werden.

Merkmale

- für Zug- und Druckkräfte
- einfache Krafteinleitung
- robuste Ausführung
- einfacher Einbau
- Schutzart IP 65 oder IP 67
- Genauigkeit 0,1% vom Endwert

Messbereich

- 0,02 kN ... 50 kN

Einsatzbereiche

- Apparatebau
- Fertigungsstraßen
- Mess- und Kontrolleinrichtungen
- Vorrichtungs- und Sondermaschinenbau
- Prüfvorrichtungen, Fertigungsanlagen etc.

besondere Hinweise

- Kontrollfunktion: 100 % Signal (optional)
- Krafteinleitungsteile optional lieferbar

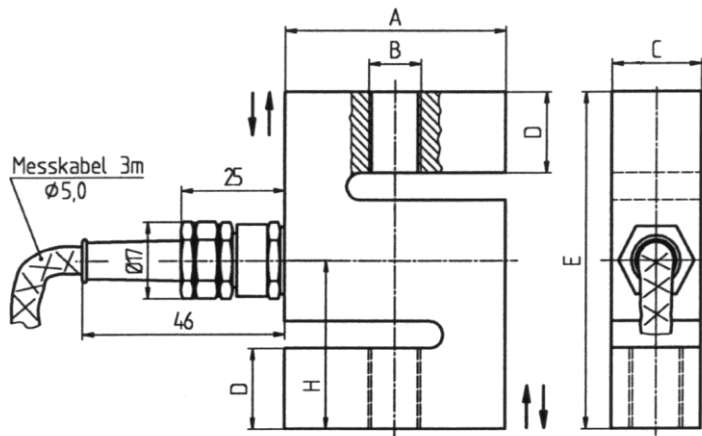
Baureihe: F2211

Technische Daten

Baureihen	F2211		Optionen
Nennkraft F_{nom} in kN kg	0,02, 0,05, 0,1, 0,2, 0,5, 1 2, 5, 10, 20, 50, 100	2, 5, 10, 20, 50 200, 500, 1000, 2000, 5000	
Grenzkraft	150% F_{nom}		
Bruchkraft	>300% F_{nom}		
zusammengesetzter Fehler	$\leq \pm 0,2\%$ v.EW.		$\leq \pm 0,1\%$ v.EW, nur bei Zug- oder Druckkraft
zulässige Schwingbreite	$\pm 70\%$ F_{nom} nach DIN 50 100		
Kriechen, 30 min. bei F_{nom}	$\leq \pm 0,07\%$ v.EW.		$\leq \pm 0,04\%$ v.EW.
Nennmessweg	<0,15 mm		
Nenntemperaturbereich	-10 bis +70°C		
Gebrauchstemperatur	-30 bis +85°C		
Lagertemperatur	-50 bis +90°C		
Referenztemperatur	23°C		
Temperatureinfluss	-Kennwert -Nullsignals	< $\pm 0,12\%$ v.EW./ 10K < $\pm 0,04\%$ v.EW./ 10K	< $\pm 0,08\%$ v.EW./10K < $\pm 0,025\%$ v.EW./10K
Schutzart (nach EN 60 529 / IEC 529)	IP 67, bis 1 kN IP 65		
Isolationswiderstand	> 2 G Ω		
Unempfindlichkeit gegen Seitenkräfte	60% vom Nennwert		
Analogausgang			
- Ausgangssignal	2 mV/V (1 mV/V bei 0,02 kN)		
- Brückenwiderstand	350 Ω		
- Option	Leitungsverstärker 0 (4) ... 20 mA, 0 ... 10 V DC		
- Kennwerttoleranz	$\leq \pm 0,1\%$ v.EW.		
- Hilfsenergie	2 ... 12 V (max. 15 V) 12 ... 28 V DC		
- elektrischer Anschluss	für Leitungsverstärker Messkabel 3 m/4-Leiter		
Kontrollfunktion			100% Signal
Überlastschutz			für Zug- + Druckkraft
Einbauhilfen für Krafteinleitung	siehe sep. Datenblatt		
Material des Messkörpers	Edelstahl, bis 1 kN Aluminium		
Gewicht (kN)			
- 0,02 – 0,05	0,25 kg		
- 0,1 - 1	0,30 kg		
- 2 - 5	0,57 kg		
- 10	0,65 kg		
- 20	1,45 kg		
- 50	1,5 kg		

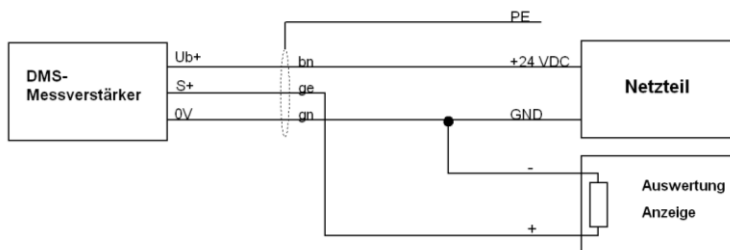
v.EW. = vom Messbereichsentwert

Maßbild



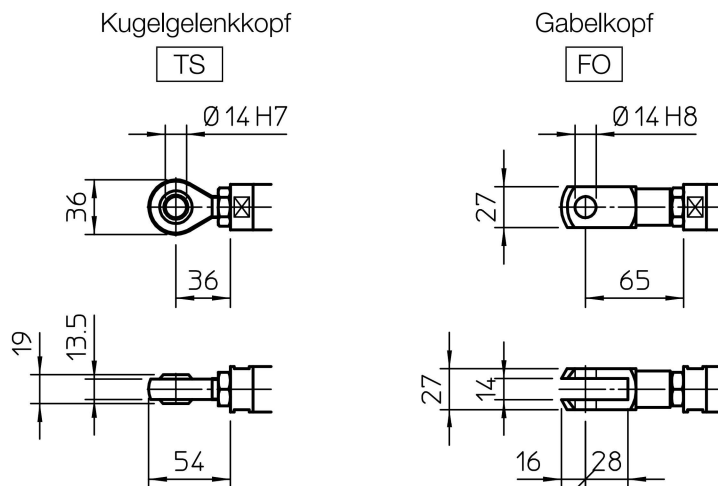
Nennkraft [kN]	Maße in [mm]					
	A	B	C	D	E	H
0,02, 0,05, 0,1, 0,2, 0,5, 1, 2, 5, 10	50	M 12.	20	18	75	37,5
20, 50	65	M 24 x 2	39,5	22	85	42,5

Elektr. Anschluss	
Vers. (-)	grün
Vers. (+)	braun
Sign. (+)	gelb
Sign.(-)	weiß
Kontrolle	grau
Schirmung	Schirm



Pinbelegung mit integriertem oder Leitungsverstärker

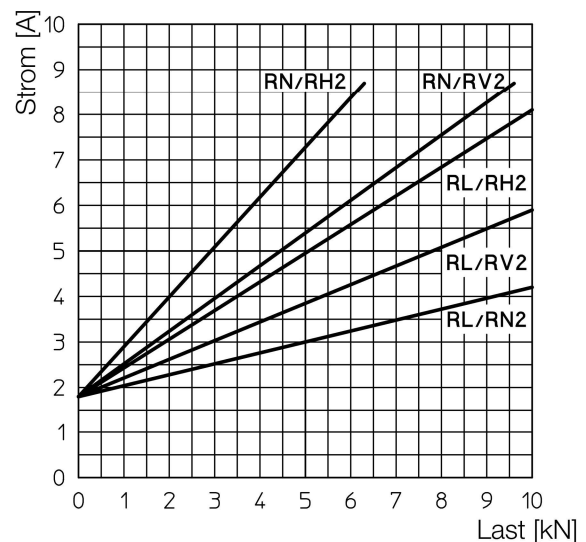
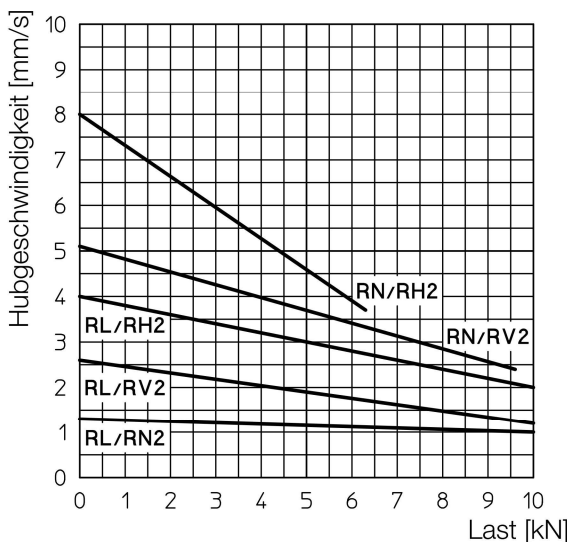
BEFESTIGUNGSKÖPFE



LEISTUNGEN mit 24 V Gleichstrommotor

(mit 12 V Gleichstrommotor: bei gleicher Last, Hubgeschwindigkeit um 10% reduziert, Stromaufnahme verdoppelt)

2-gängige Trapezspindel Tr 18x8 (P4)



LEISTUNGEN mit Drehstrommotor 50 Hz 230/400 V oder Wechselstrommotor 50 Hz 230 V

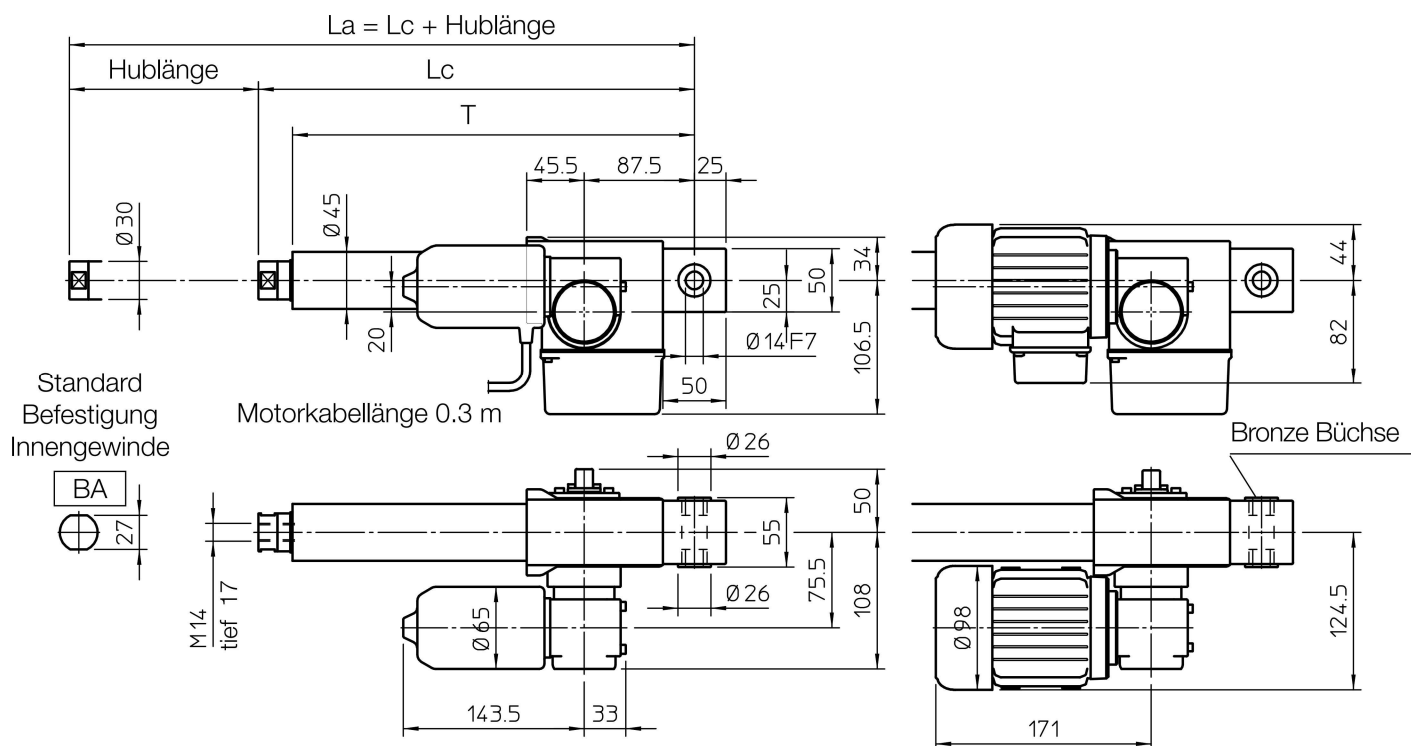
2-gängige Trapezspindel Tr 18x8 (P4)		
UNTERSETZUNG	Motor 0.06 kW - 2 polig	
	LAST [N]	V _{HUB} [mm/s]
RL/RH2	3600	3.7
RL/RV2	5500	2.4
RL/RN2	9600	1.2

Statische Selbsthemmung

Hinweise zur statischen Selbsthemmung bei Zug- oder Drucklast siehe Seite 68.

BESTELLBEISPIEL

CLA 28	RL1	C800	DC 24 V	FC2	POR 5K			
Antrieb	Unter- setzung	Hublänge	Motor	Endschalter	Zubehör		Optionen	

ABMESSUNGEN


Abmessungen [mm]	
Lc [mm]	230 + Hub
T [mm]	191 + Hub

LEISTUNGEN UND EIGENSCHAFTEN

- Zug- und Drucklast bis zu 10.000 N
- Hubgeschwindigkeit bis zu 8 mm/s (DC Motor)
- Hubgeschwindigkeit bis zu 3,7 mm/s (AC Motor)
- Standardhublänge:
200, 300, 400, 500, 600, 700, 800 mm
(für Sonderhublängen bitte kontaktieren Sie uns)
- Gehäuse aus Gusseisen mit integriertem hinterem Anschluss und Bronze Büchse
- Schutzrohr aus eloxiertem Aluminium
- Schubrohr aus verchromtem Stahl - Toleranz f7
- Vorderer Befestigungsanschluss BA aus rostfreiem Stahl AISI 303
- Motoren (technische Details Seite 69 und 70):
- 12, 24, oder 36 V Gleichstrommotoren mit elektromagnetischem Geräuschfilter
- Drehstrommotor oder Wechselstrommotor
- Einschaltdauer bei max. Last:
- DC Motor max. 15% je 10 Minuten bei (-10 ... +40)°C
- AC Motor max. 30% je 10 Minuten bei (-10 ... +40)°C
- Schutzklasse:
- mit Gleichstrommotor IP 65
Test IP6X gemäß EN 60529 §12 §13.4-13.6
Test IPX5 gemäß EN 60529 §14.2.5
- mit AC Motor ohne Bremse IP 55
- mit AC Motor mit Bremse IP54
(Antriebe wurden im Stillstand getestet)

- Standard Motor- und Vorschaltgetriebeanbauposition wie oben dargestellt (rechte Ausführung, Bestellcode RH)
- Lebensgeschmiert, wartungsfrei

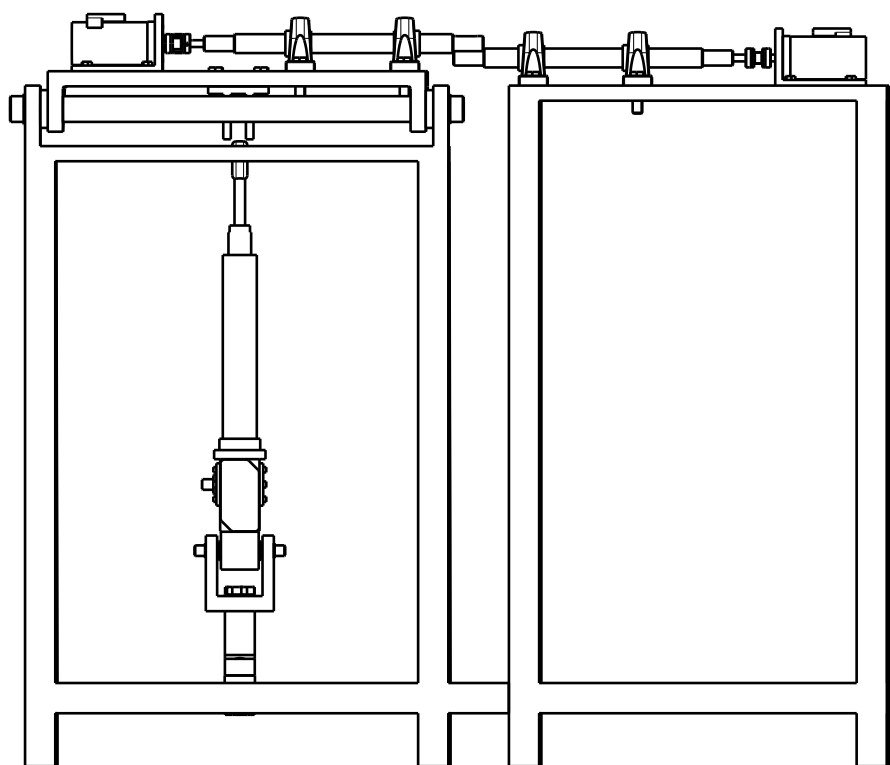
ZUBEHÖR

- Verschiedene vordere Befestigungsanschlüsse
- Schubrohr aus rostfreiem Stahl AISI 304 (Bestellcode SS)
- Mechanischer Schutz gegen dynamische Überlast: Rutschkupplung (Bestellcode FS)
- Verdrehsicherung (Bestellcode AR)
- Einstellbare, elektrische Endschalter (Bestellcode FC2)
- Einstellbare, elektrische Endschalter, die den Motor direkt abschalten (nicht mit Drehstrommotor verfügbar) (Bestellcode FC2X)
- Dritter Endschalter für mittleres Positionssignal (Code FC)
- Rotatives Potentiometer 5kOhm zur Positionskontrolle (Bestellcode POR5K)

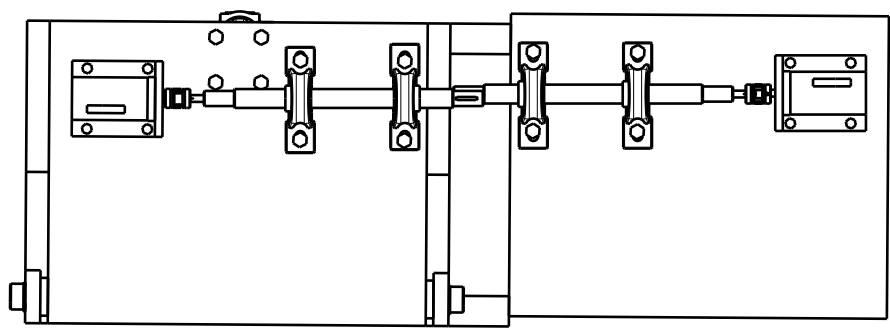
ACHTUNG: der dritte Schalter und das Potentiometer können nicht zusammen geliefert werden.

OPTIONEN

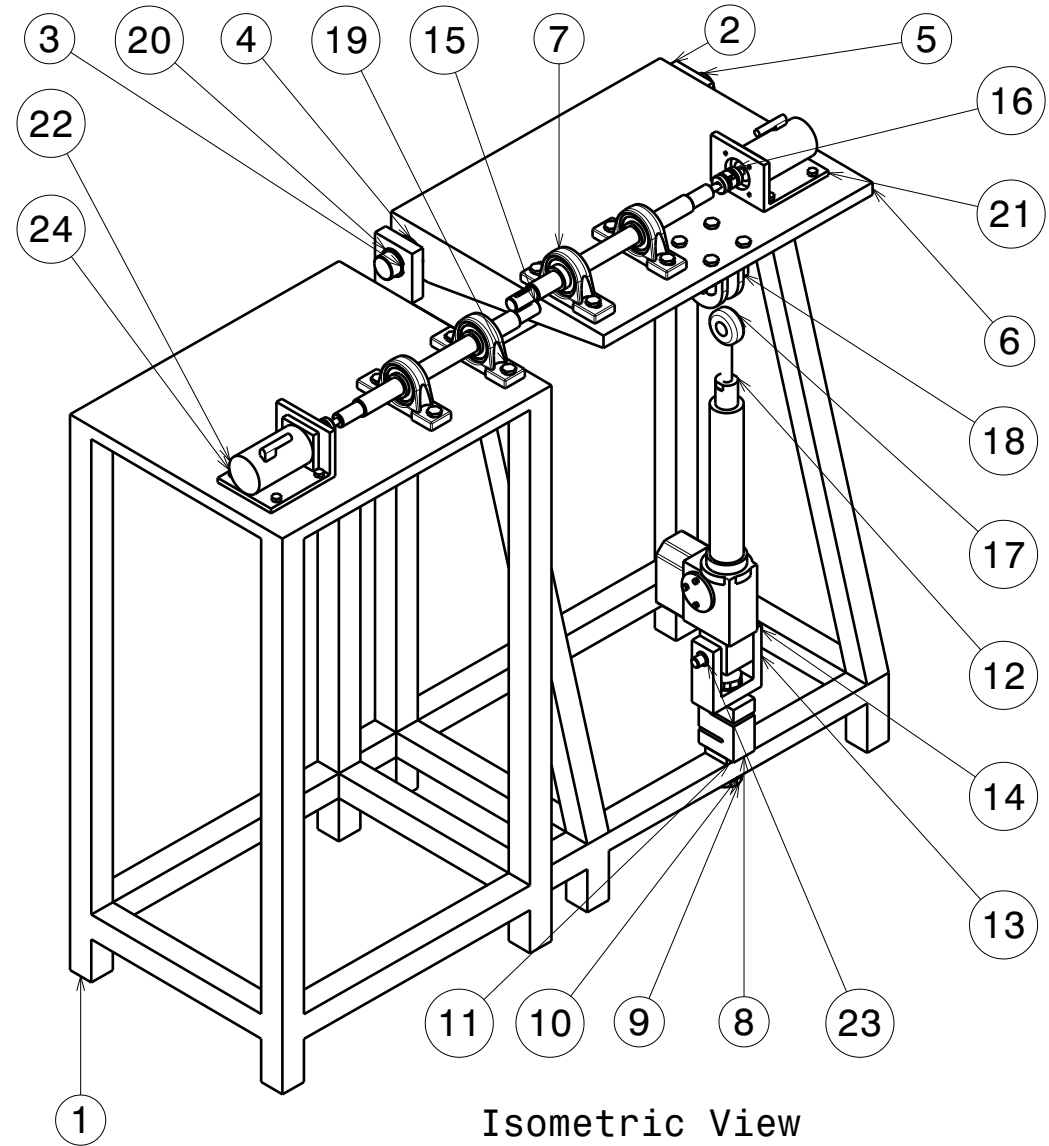
- Elektromotor- und Vorschaltgetriebeanbau um 180° drehbar (linke Ausführung, Bestellcode LH)



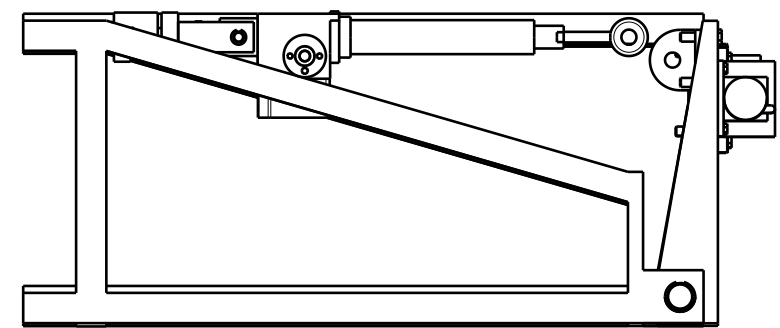
Frontview
Scale: 1:10



Topview
Scale: 1:10



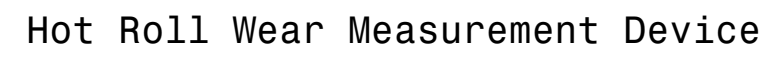
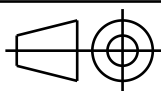
Isometric View
Scale: 1:10



Sideview left
Scale: 1:10

Bill of materials

Nr.	Name	Quantity
1	Table Hot Strip	1
2	Table Sample Bottom	1
3	Bearing Bush	2
4	Table Shaft Ring	2
5	Table Shaft	1
6	Table Sample Top	1
7	Bearing/Bearing Housing	4
8	Force Sensor teccis F2211	1
9	M24 Screw	1
10	M24 Screw Protector Ring	1
11	Force Sensor Ring Bottom	1
12	Actuator Linearmech CLA28	1
13	Actuator Connector	1
14	Bolt Ring	1
15	Sample Shaft	2
16	Coupling Rotex GS	2
17	Table Actuator Holder (Comes with the Linear Actuator CLA28)	1
18	Table Actuator Connector	1
19	M12 Screw	12
20	Shaft Disk	2
21	M6 Screw	8
22	Engine 8LSA73	2
23	Bolt	1
24	Engine Holder	2

DESIGNED BY: Alain Tran			I	-
DATE: June 2017			H	-
CHECKED BY: XXX			G	-
DATE: XXX			F	-
SIZE: A3		DRAWING NUMBER	E	-
SCALE: 1:10	WEIGHT (kg)		C	-
		SHEET	B	-
			A	-



Hot Roll Wear Measurement Device

1/1

This drawing is our property; it can't be reproduced or communicated without our written agreement.

D

C

B

A

4

4

3

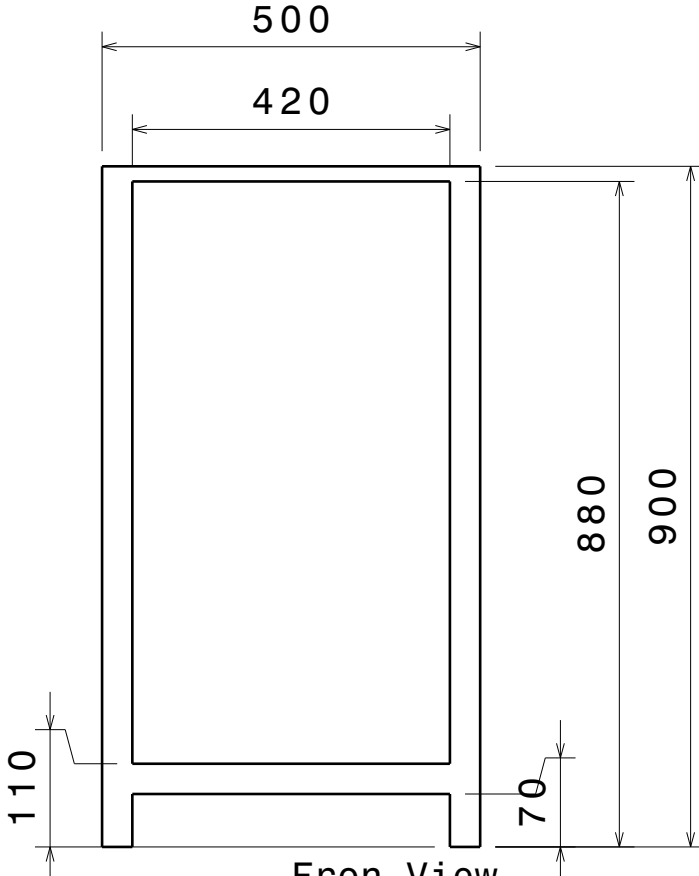
3

2

2

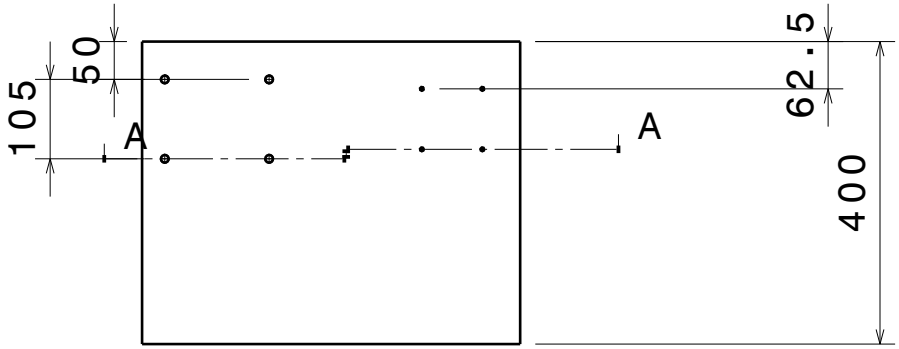
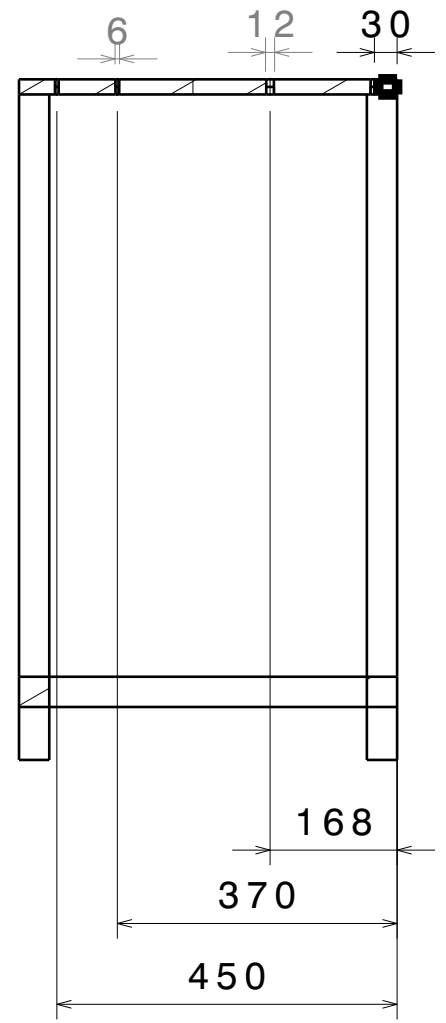
1

1



Fron View
Scale: 1:10

Cut A-A
Scale: 1:10



Top View
Scale: 1:10

DESIGNED BY:
Alain Tran
DATE:
June 2017

CHECKED BY:
XXX
DATE:
XXX

SIZE
A4

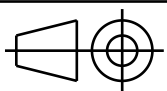


Table Hot Strip

SCALE
1:10

WEIGHT (kg)
1

DRAWING NUMBER
1

SHEET
1 / 1

I	-
H	-
G	-
F	-
E	-
D	-
C	-
B	-
A	-

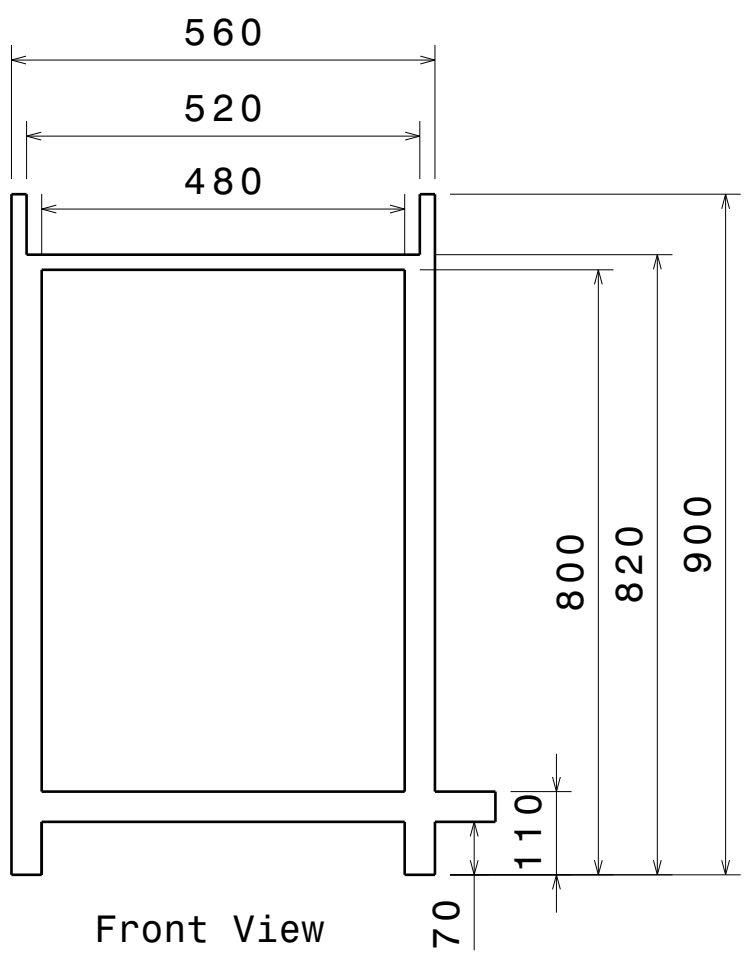
This drawing is our property; it can't be reproduced or communicated without our written agreement.

D

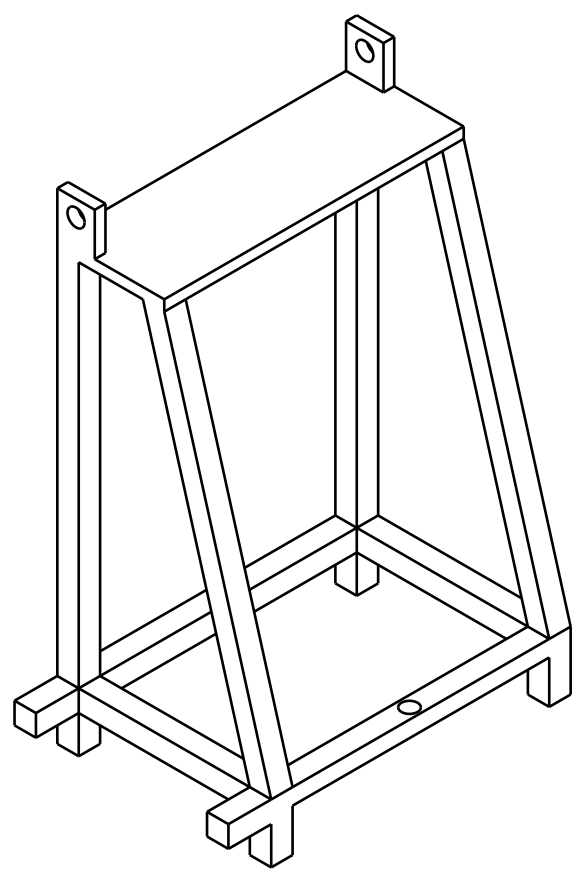
A

D C B A

4



Front View
Scale: 1:10



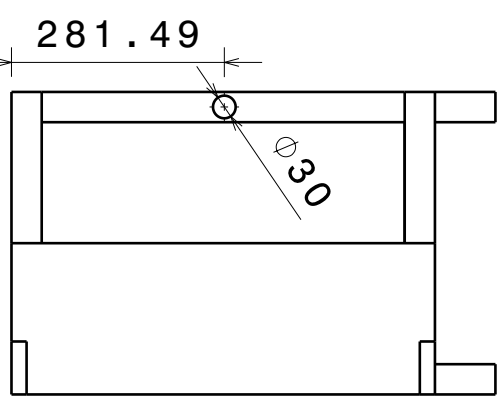
Isometric View
Scale: 1:10

3

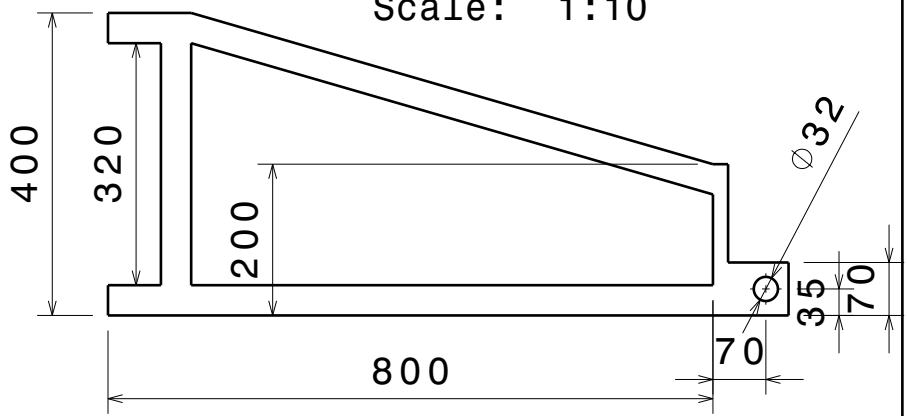
3

2

2



Top View
Scale: 1:10



Side View Left
Scale: 1:10

1

1

DESIGNED BY:
Alain Tran
DATE:
June 2017
CHECKED BY:
XXX
DATE:
XXX

SIZE
A4

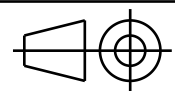


Table Sample Bottom

SCALE
1:10

WEIGHT (kg)

DRAWING NUMBER
2

SHEET
1 / 1

I	-
H	-
G	-
F	-
E	-
D	-
C	-
B	-
A	-

This drawing is our property; it can't be reproduced or communicated without our written agreement.

D A

D

C

B

A

4

4

3

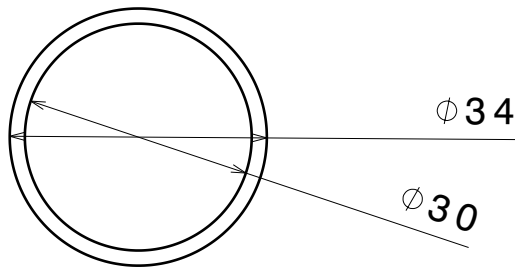
3

2

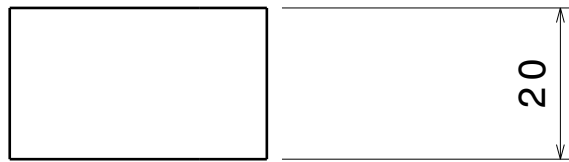
2

1

1



Bottom View
Scale: 1:1

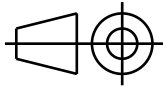


Front View
Scale: 1:1

DESIGNED BY:
Alain Tran
DATE:
June 2017

CHECKED BY:
XXX
DATE:
XXX

SIZE
A4



Bearing Bush

SCALE
1:1

WEIGHT (kg)

DRAWING NUMBER
3

SHEET
1 / 1

I	-
H	-
G	-
F	-
E	-
D	-
C	-
B	-
A	-

This drawing is our property; it can't be reproduced or communicated without our written agreement.

D

A

D

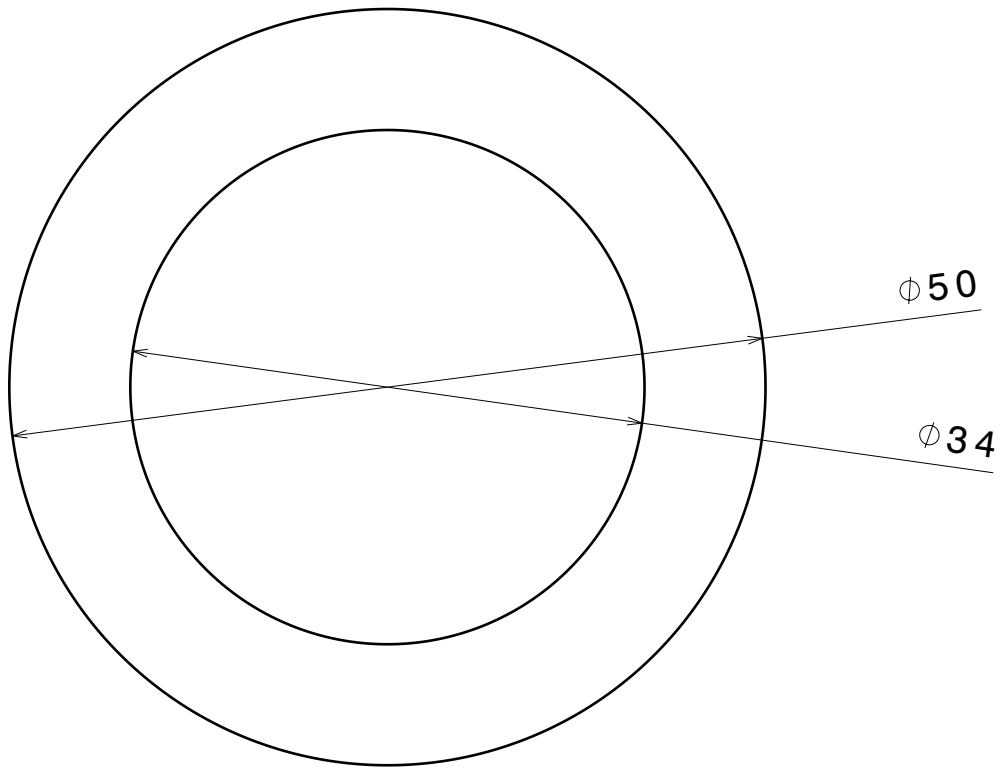
C

B

A

4

4



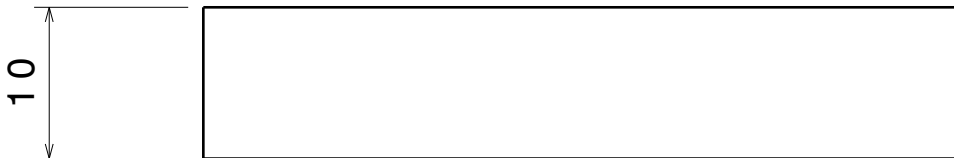
3

3

Top View
Scale: 2:1

2

2



Front View
Scale: 2:1

1

1

DESIGNED BY: Alain Tran		<h1>Table Shaft Ring</h1>		I	-
DATE: June 2017				H	-
CHECKED BY: XXX				G	-
DATE: XXX		F	-		
SIZE A4		E	-		
SCALE 2:1	WEIGHT (kg)	D	-		
DRAWING NUMBER 4		C	-		
SHEET 1 / 1		B	-		
This drawing is our property; it can't be reproduced or communicated without our written agreement.		A	-		

D

A

D

C

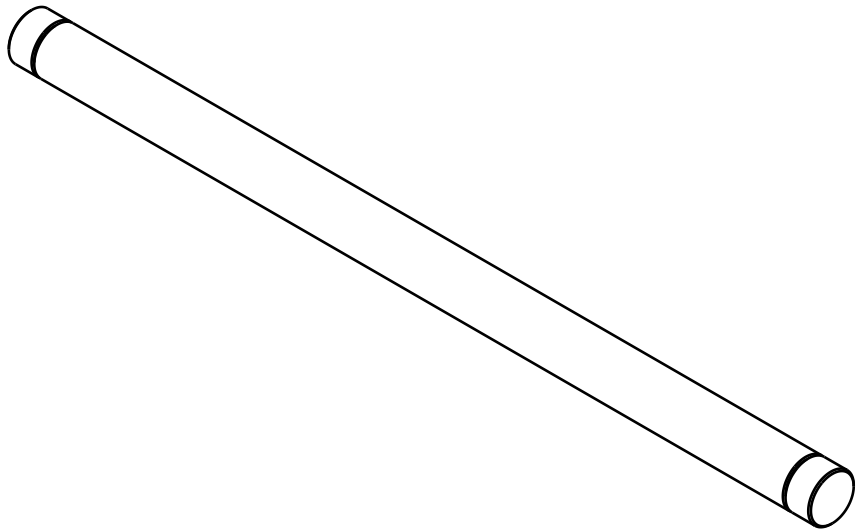
B

A

4

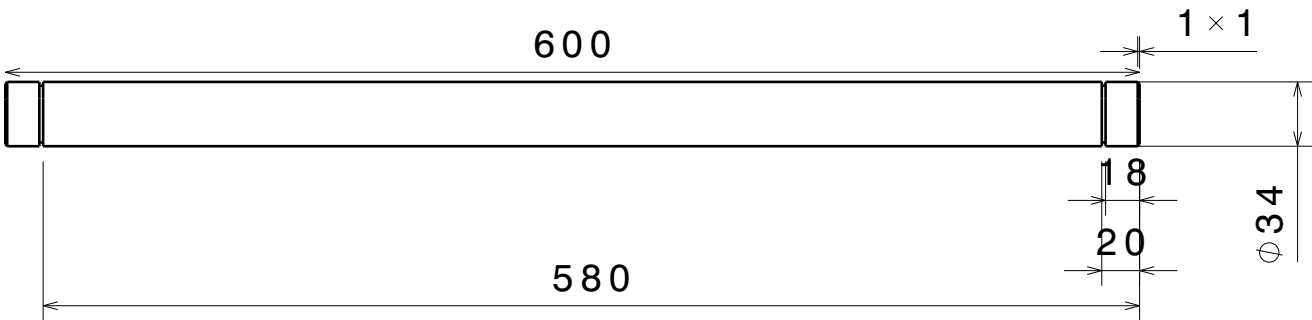
4

Isometric View
Scale: 1:4



3

3



Front View
Scale: 1:4

2

2

1

1

DESIGNED BY:
Alain Tran

DATE:
June 2017

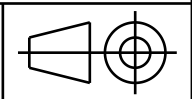
CHECKED BY:
XXX

DATE:
XXX

Table Shaft

I	-
H	-
G	-
F	-
E	-
D	-
C	-
B	-
A	-

SIZE
A4



SCALE
1:4

WEIGHT (kg)

DRAWING NUMBER
5

SHEET
1 / 1

This drawing is our property; it can't be reproduced or communicated without our written agreement.

D

A

D

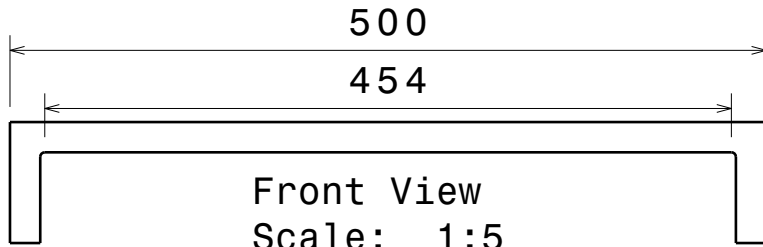
C

B

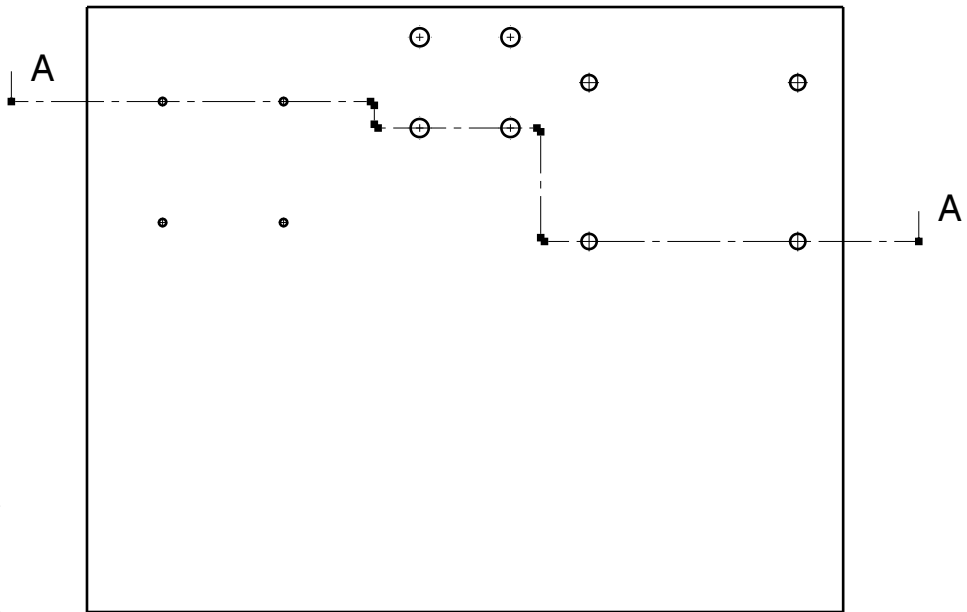
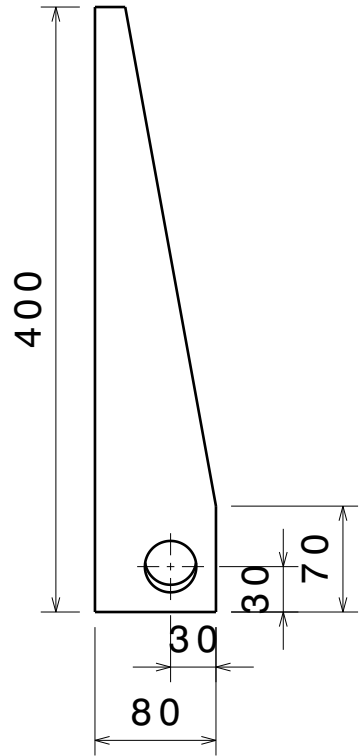
A

4

4



20



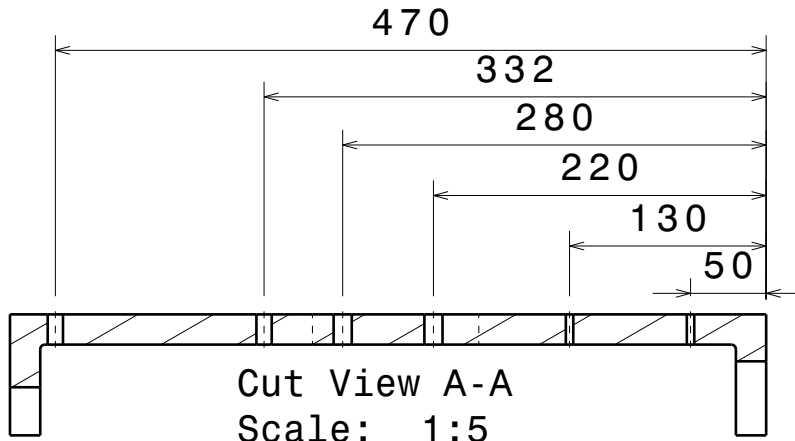
Top View
Scale: 1:5

3

3

2

2



Cut View A-A
Scale: 1:5

DESIGNED BY:
Alain Tran

DATE:
June 2017

CHECKED BY:
XXX

DATE:
XXX

SIZE
A4

SCALE
1:5

Table Sample Top

WEIGHT (kg)
6

DRAWING NUMBER
6

SHEET
1 / 1

I	-
H	-
G	-
F	-
E	-
D	-
C	-
B	-
A	-

1

1

This drawing is our property; it can't be reproduced or communicated without our written agreement.

D

A

D

C

B

A

4

4

3

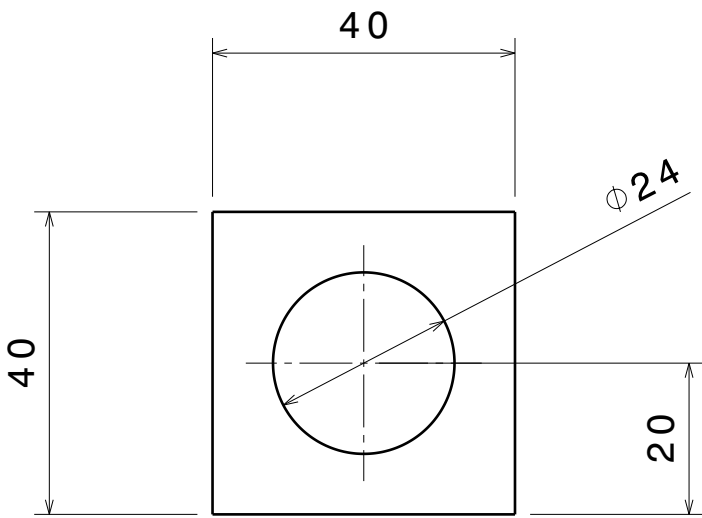
3

2

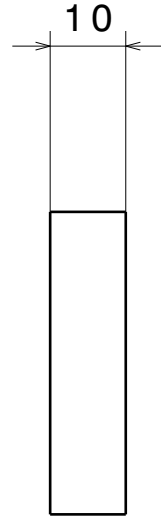
2

1

1



Side View Right
Scale: 1:1

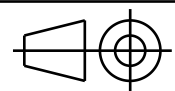


Front View
Scale: 1:1

DESIGNED BY:
Alain Tran
DATE:
June 2017

CHECKED BY:
XXX
DATE:
XXX

SIZE
A4



Force Sensor Ring Bottom

SCALE
1:1

WEIGHT (kg)

DRAWING NUMBER
11

SHEET
1 / 1

I	-
H	-
G	-
F	-
E	-
D	-
C	-
B	-
A	-

This drawing is our property; it can't be reproduced or communicated without our written agreement.

D

A

D

C

B

A

4

4

3

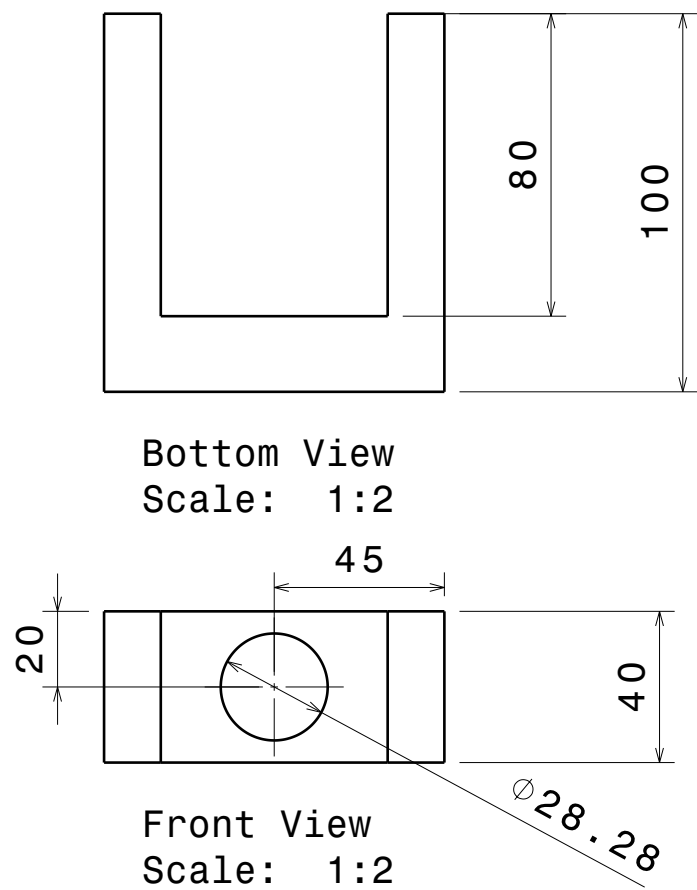
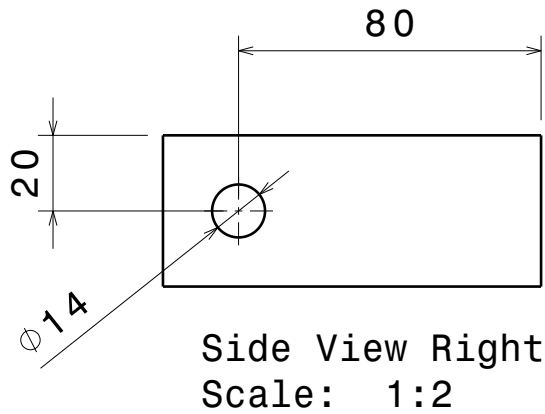
3

2

2

1

1



DESIGNED BY: Alain Tran	
DATE: June 2017	
CHECKED BY: XXX	
DATE: XXX	
SIZE A4	
SCALE 1:2	WEIGHT (kg)

Actuator Connector	
SHEET 1 / 1	

I	-
H	-
G	-
F	-
E	-
D	-
C	-
B	-
A	-

This drawing is our property; it can't be reproduced or communicated without our written agreement.

D

A

D

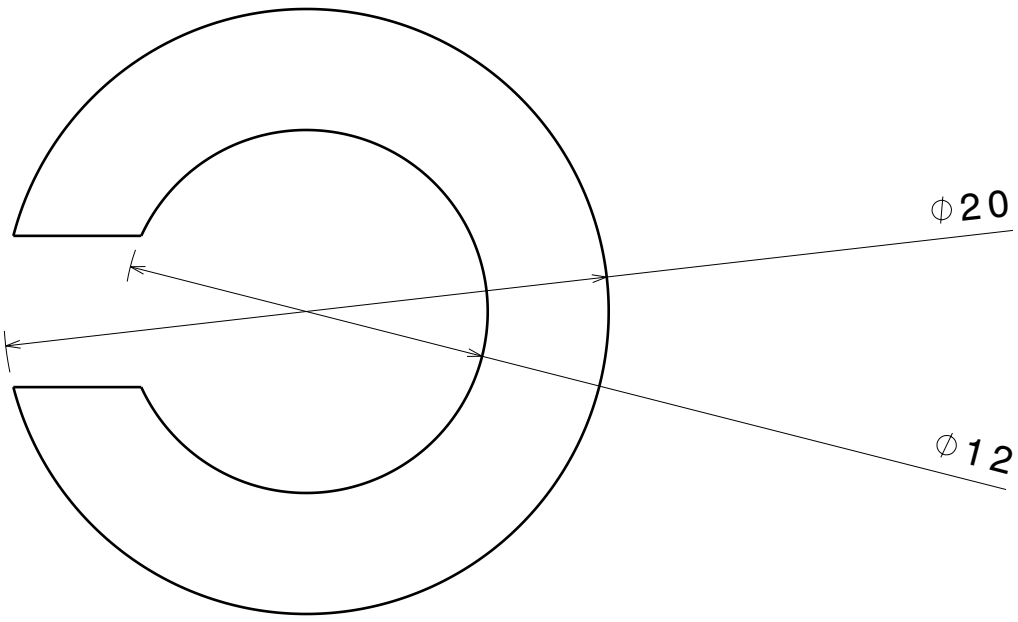
C

B

A

4

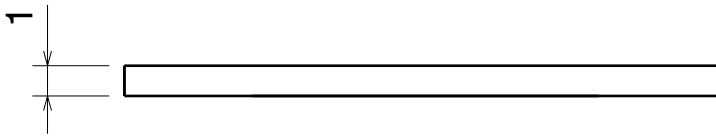
4



Top View
Scale: 4:1

3

3



Front View
Scale: 4:1

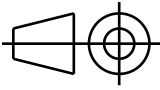
2

2

DESIGNED BY:
Alain Tran
DATE:
June 2017

CHECKED BY:
XXX
DATE:
XXX

SIZE
A4



Bolt Ring

SCALE
4:1

WEIGHT (kg)

DRAWING NUMBER
14

SHEET
1 / 1

I	-
H	-
G	-
F	-
E	-
D	-
C	-
B	-
A	-

1

1

This drawing is our property; it can't be reproduced or communicated without our written agreement.

D

A

D

C

B

A

4

4

3

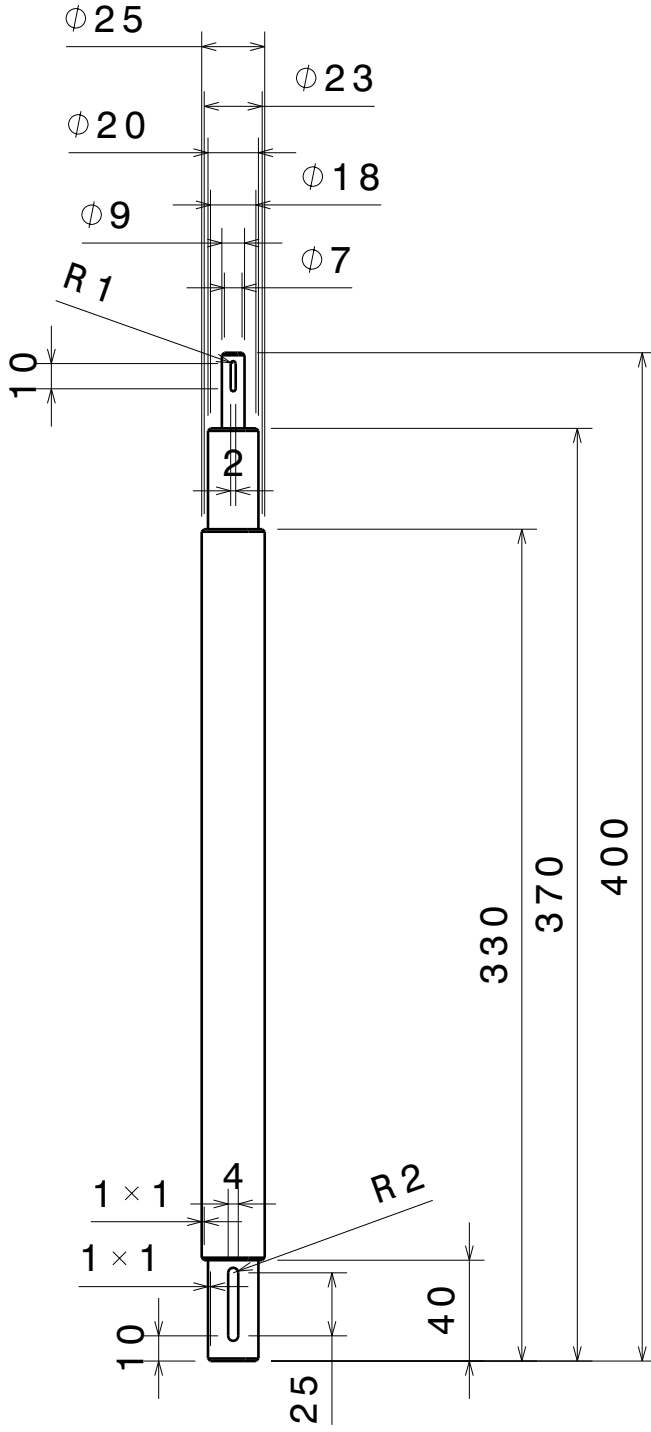
3

2

2

1

1

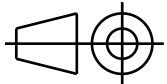


Front View
Scale: 1:3

DESIGNED BY:
Alain Tran
DATE:
June 2017

CHECKED BY:
XXX
DATE:
XXX

SIZE
A4



Sample Shaft

SCALE
1:2

WEIGHT (kg)

DRAWING NUMBER
15

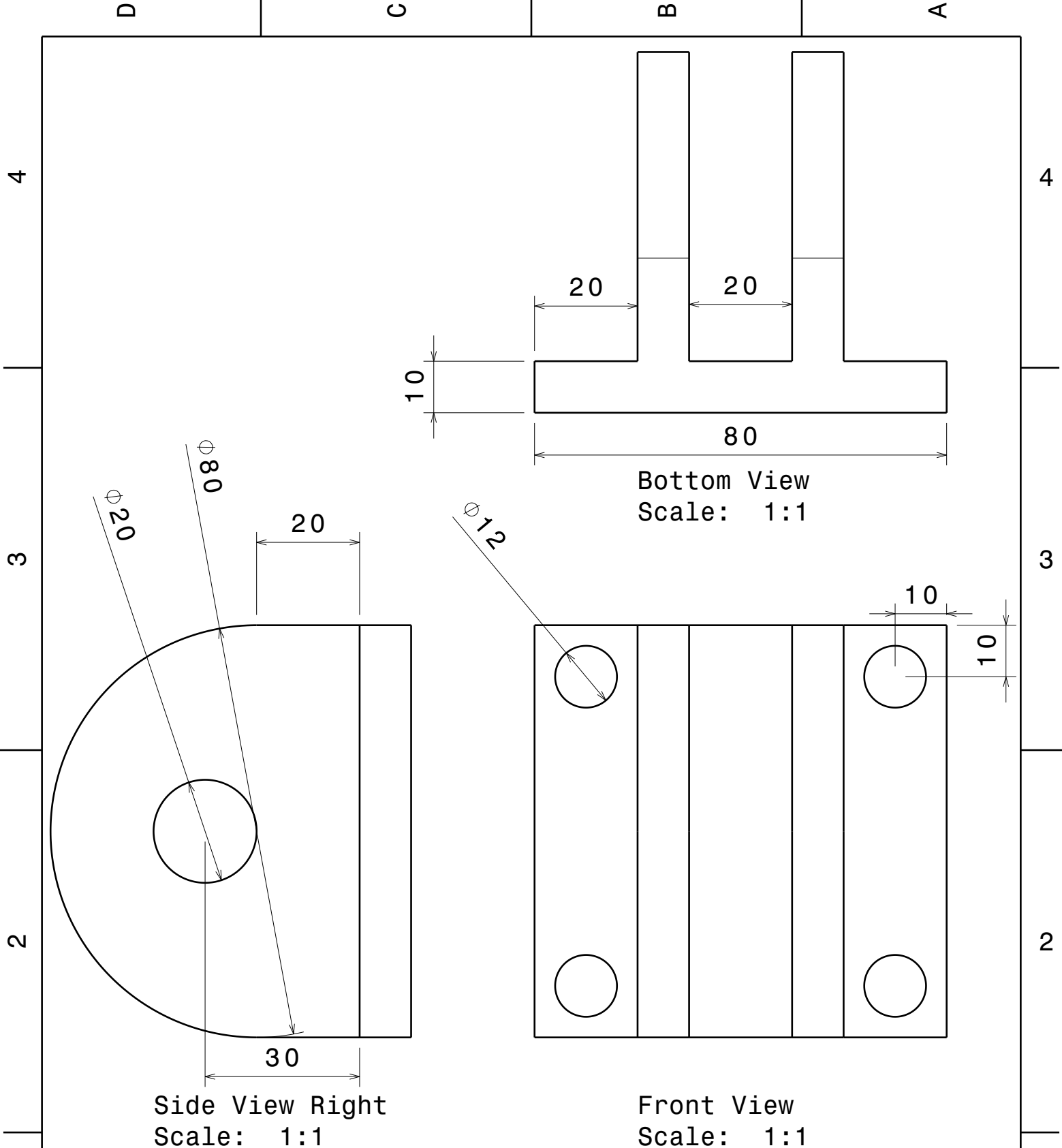
SHEET
1 / 1

I	-
H	-
G	-
F	-
E	-
D	-
C	-
B	-
A	-

This drawing is our property; it can't be reproduced or communicated without our written agreement.

D

A



DESIGNED BY:
Alain Tran

DATE:
June 2017

CHECKED BY:
XXX

DATE:
XXX

SIZE
A4

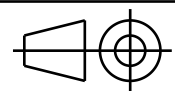


Table Actuator Connector

SCALE
1:1

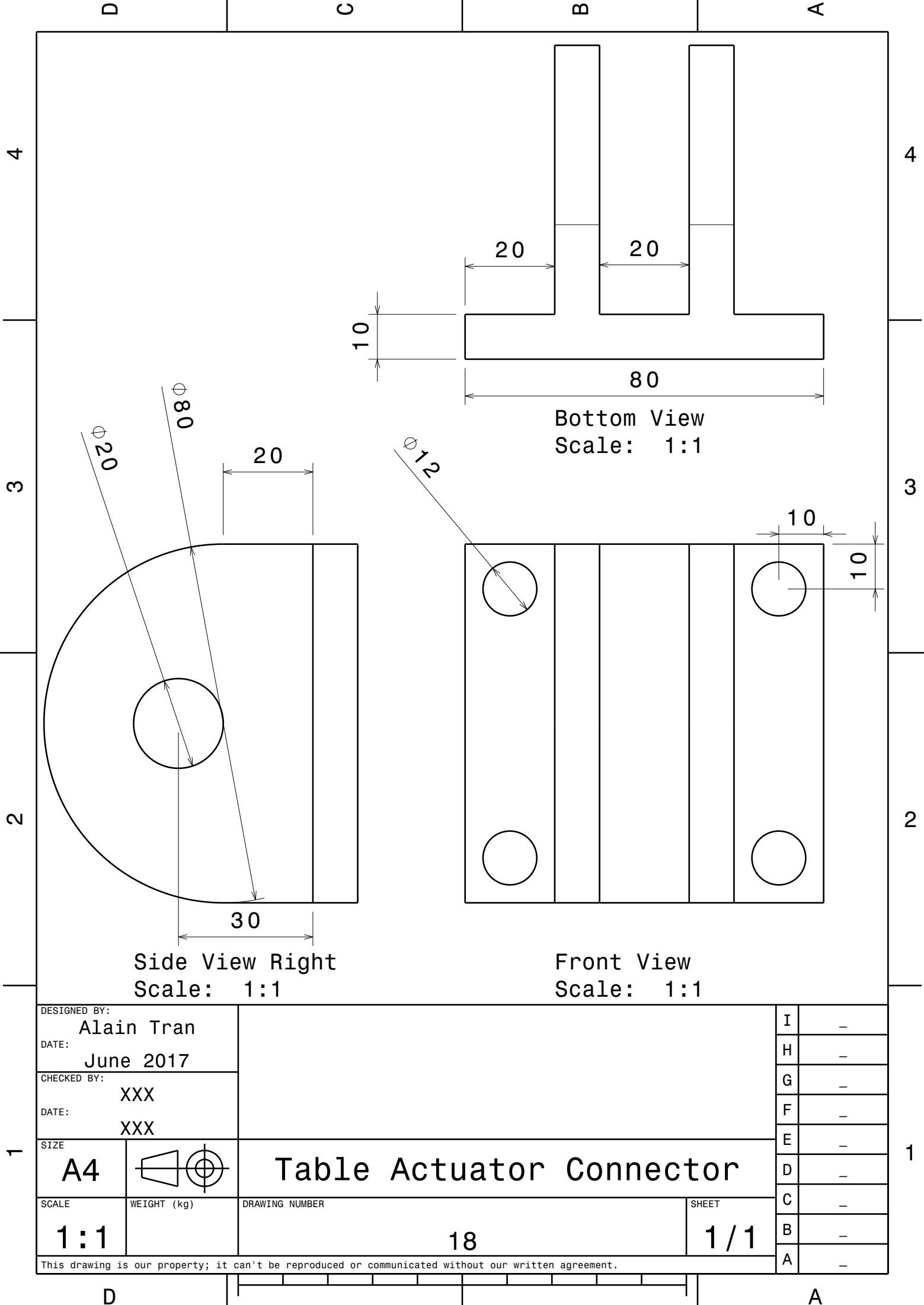
WEIGHT (kg)

DRAWING NUMBER
18

SHEET
1 / 1

I	-
H	-
G	-
F	-
E	-
D	-
C	-
B	-
A	-

This drawing is our property; it can't be reproduced or communicated without our written agreement.



D

C

B

A

4

4

3

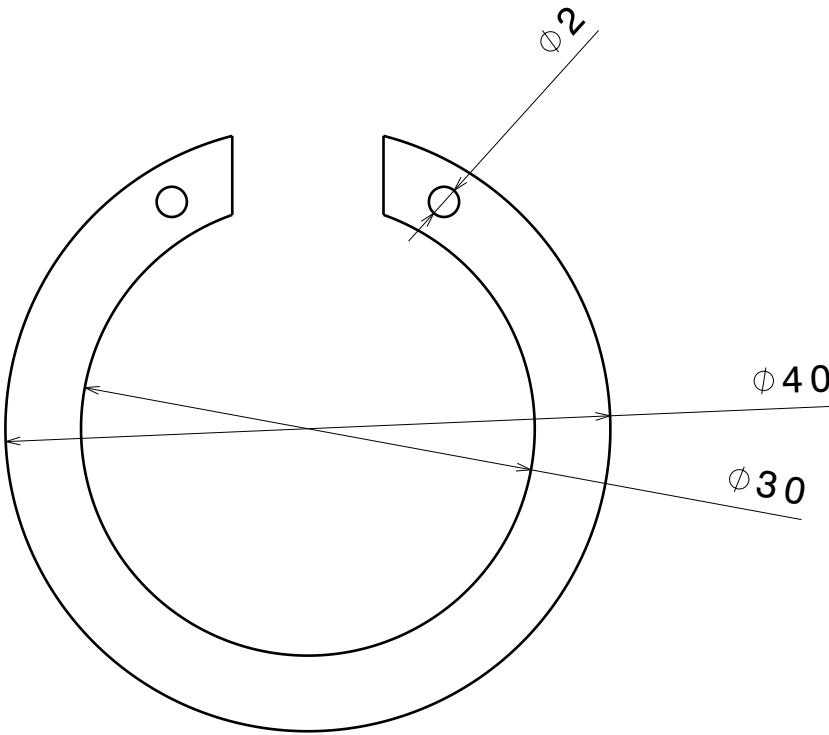
3

2

2

1

1



Front View
Scale: 2:1

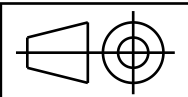
Side View Left
Scale: 2:1

DESIGNED BY:
Alain Tran
DATE:
June 2017
CHECKED BY:
XXX
DATE:
XXX

Shaft Disk

I	-
H	-
G	-
F	-
E	-
D	-
C	-
B	-
A	-

SIZE
A4



SCALE
2:1

WEIGHT (kg)

DRAWING NUMBER
20

SHEET
1 / 1

This drawing is our property; it can't be reproduced or communicated without our written agreement.

D

A

D

C

B

A

4

4

1 x 1

14

4

5

60

65

3

3

2

2

Front View
Scale: 3:2

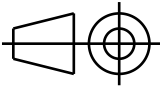
1

1

DESIGNED BY:
Alain Tran
DATE:
June 2017

CHECKED BY:
XXX
DATE:
XXX

SIZE
A4



Bolt

SCALE
1:2

WEIGHT (kg)

DRAWING NUMBER
23

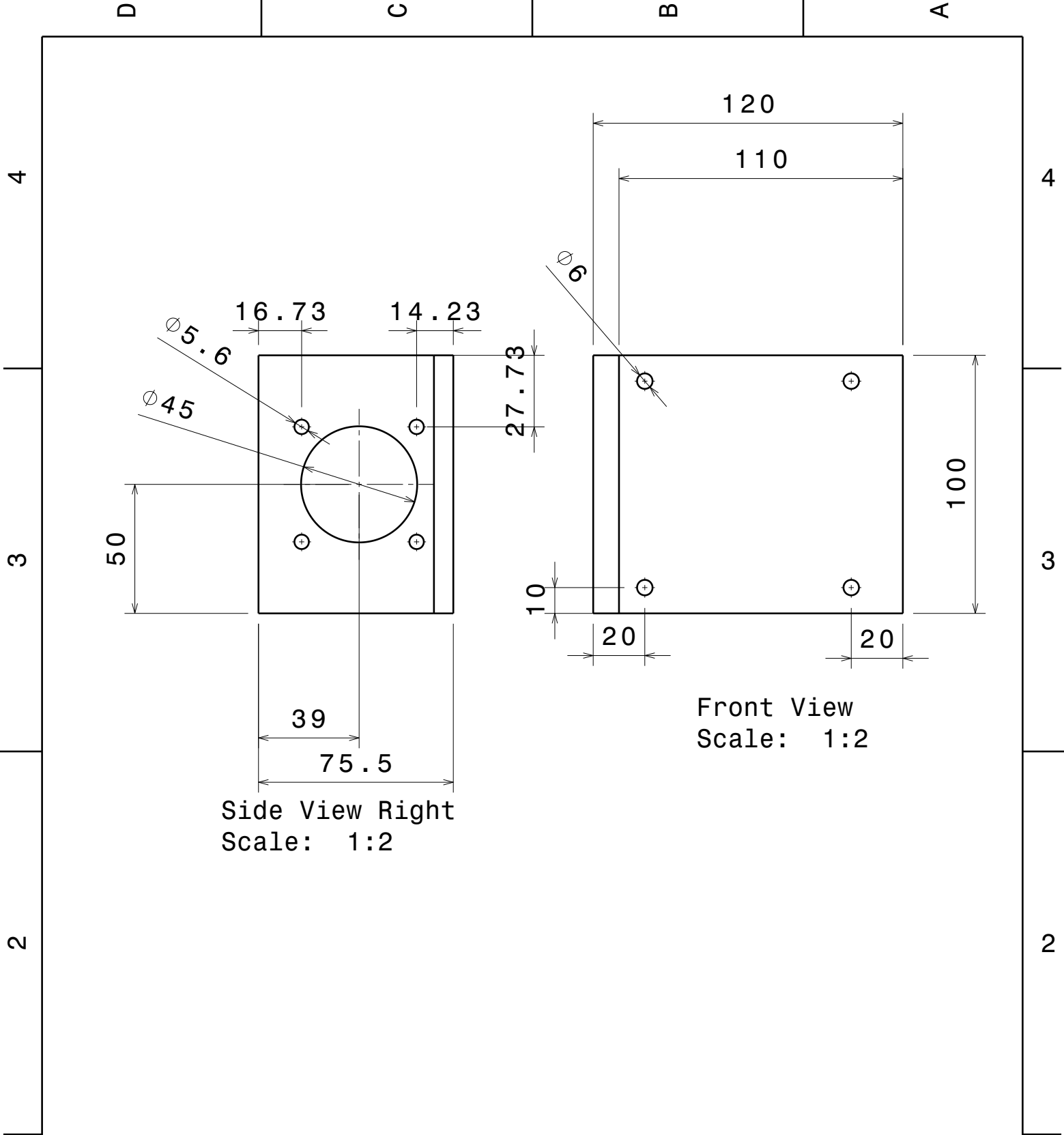
SHEET
1 / 1

I	-
H	-
G	-
F	-
E	-
D	-
C	-
B	-
A	-

This drawing is our property; it can't be reproduced or communicated without our written agreement.

D

A



DESIGNED BY: Alain Tran				I	-
DATE: June 2017				H	-
CHECKED BY: XXX				G	-
DATE: XXX				F	-
SIZE A4		Engine Holder		E	-
SCALE 1:2	WEIGHT (kg)			D	-
DRAWING NUMBER 24		SHEET 1 / 1		C	-
				B	-
				A	-

This drawing is our property; it can't be reproduced or communicated without our written agreement.